

1 **Intercomparison of detection and quantification methods for methane emissions from**
2 **the natural gas distribution network in Hamburg, Germany**

3
4 Hossein Maazallahi^{1, 2}, Antonio Delre³, Charlotte Scheutz³, Anders M. Fredenslund³, Stefan
5 Schwietzke⁴, Hugo Denier van der Gon², Thomas Röckmann¹

6
7 ¹*Institute for Marine and Atmospheric research Utrecht (IMAU), Utrecht University (UU),*
8 *Utrecht, The Netherlands*

9 ²*Netherlands Organisation for Applied Scientific Research (TNO), Utrecht, the Netherlands*

10 ³*Department of Environmental Engineering, Technical University of Denmark (DTU),*
11 *Lyngby, Denmark*

12 ⁴*Environmental Defense Fund (EDF), Berlin, Germany*

13
14 **Correspondence:** Hossein Maazallahi (h.maazallahi@uu.nl)

15
16 **Abstract:**

17 In August and September 2020, three different measurement methods for quantifying methane
18 (CH₄) emission from leaks in urban gas distribution networks were applied and compared in
19 Hamburg, Germany: the “mobile”, “tracer release” and “suction” methods.
20 The mobile and tracer release methods determine emission rates to the atmosphere from
21 measurements of CH₄ mole fractions in the ambient air, and the tracer release method also
22 includes measurement of a gaseous tracer. The suction method determines emission rates by
23 pumping air out of the ground using soil probes that are placed above the suspected leak
24 location. The quantitative intercomparison of the emission rates from the three methods at a
25 small number of locations is challenging because of limitations of the different methods at
26 different types of leak locations.

27 The mobile method was designed to rapidly quantify the average or total emission rate of many
28 gas leaks in a city, but it yields a large emission rate uncertainty for individual leak locations.
29 Emission rates determined for individual leak locations with the tracer release technique are
30 more precise because the simultaneous measurement of the tracer released at a known rate at
31 the emission source eliminates many of the uncertainties encountered with the mobile method.
32 Nevertheless, care must be taken to properly collocate the tracer release and the leak emission
33 points to avoid biases in emission rate estimates. The suction method could not be completed
34 or applied at locations with widespread subsurface CH₄ accumulation, or due to safety
35 measures, and this sampling bias may be associated with a bias towards leak locations with low
36 emission rates. The leak locations where the suction method could not be applied were the
37 biggest emitters as confirmed by the emission rate quantifications using mobile and tracer
38 methods and an engineering method based on leak’s diameter, pipeline overpressure and depth
39 at which the pipeline is buried. The corresponding sampling bias for the suction technique led
40 to a low bias in derived emission rates in this study. It is important that future studies using the
41 suction method account for any leaks not quantifiable with this method in order to avoid biases,
42 especially when used to inform emission inventories.

1 Introduction

Natural gas combustion has a lower carbon footprint than combustion of other fossil fuel sources for the same thermal output (EIA, 2021). However, fugitive methane (CH₄) emissions can significantly turn the balance in terms of climate impact (Alvarez et al., 2012) because the global warming potential of CH₄ over a 20-year time scale is 84 times higher than that of carbon dioxide (CO₂) (Myhre et al., 2013). The atmospheric abundance of CH₄ has increased about 2.5-fold since the pre-industrial era (Bousquet et al., 2006). Following a short period of stable levels after the year 2000, atmospheric CH₄ has continued to increase since 2006. Worden et al (2017) concluded that about 50 to 80% of the post-2006 increase originated from fossil sources and Jackson et al. (2020) attributed the accelerated increase of 6 – 13 ppb yr⁻¹ from 2014 to 2017 (Nisbet et al., 2019), equally to the emission increase from fossil and agriculture sectors.

Gas distribution networks in cities are subject to maintenance programs by the operators to detect and fix leakages that occur, as CH₄ is an incendiary gas and can be explosive at concentrations between 4 and 16% in ambient air (DVGW, 2022). Since the safe operation of the distribution network and leak repair is the primary objective of this maintenance, quantification of emissions from leakages is rarely performed. The absence of regulations on CH₄ emissions is another reason why leak rates are not routinely quantified, however CH₄ emissions from the energy sector needs to be addressed properly within the EU CH₄ strategy by 2050 (EC, 2020). Nevertheless, from the perspective of climate change and possible mitigation options, it is important that emissions from gas leakages are (i) quickly detected and fixed and (ii) well quantified. Weller et al. (2020) and Alvarez et al. (2018) respectively reported 5 and 1.6 times higher CH₄ emissions from leaks in the US gas distribution network based on such observations compared to the national inventory reports.

Leaks from buried pipelines can be due to corrosion or failure/defects in joints or materials (EPA, 1996). When a leak occurs on a buried urban gas pipeline, the gas will generally accumulate in the air space below the surface and then find its path to the atmosphere through a single or several surface outlets. The outlets can be either unpaved soil surfaces, cracks in the road or pavements, or associated with different types of cavities (manholes, communication covers, rain drains, etc.). The major outlet is generally the one with the highest overall permeability for gas released from the buried natural gas pipeline. On the way from the leak location on a buried pipeline to the atmosphere through outlets, CH₄ may be oxidized by methanotrophs in the soil and/or merge with CH₄ from other sources, e.g. biogenic CH₄ emissions from sewage system.

Routine leak surveys in Germany are conducted by walking with handheld CH₄ sensors above buried pipelines, referred to as the carpet method (DVGW, 2019). The success of leak detection with the carpet method depends primarily on soil permeability (Ulrich et al., 2019), which is influenced by soil moisture, texture, soil organic content and the location of the groundwater table (Wiesner et al., 2016). Based on risk of explosion, gas leaks are classified into four types: A1, A2, B and C (DVGW, 2019). This classification is based on the accumulation of CH₄ in cavities (e.g. manholes, rain drains, etc.) or buildings and the distance of gas leaks to buildings and cavities. If natural gas leaks into buildings or cavities, the leak classifies as A1, and it must be repaired immediately to minimize explosion risk. If the gas leak has a distance up to 1 m to buildings and does not fill cavities, it is classified as A2, and it must be fixed within a week. If the distance is between 1 to 4 m to buildings, the leak is classified as B and the repair time

97 window is three months, and if the distance is more than 4 m then, the leak is considered as C
98 category and can be fixed according to the scheduled repair plan. *There are 6,500 km of low*
99 *pressure and 250 km of medium pressure gas pipelines in Hamburg which are monitored*
100 *every 4 years with the carpet method based on the national regulations in Germany. Gas*
101 *leaks in cities are not quantified and thus also not a parameter affecting the course of action.*
102 *Moreover, high pressure pipelines are monitored on annual basis with additional helicopter-*
103 *based measurement platform.*

104
105 In recent years, mobile measurement methods using vehicles with fast and high-precision laser
106 instrumentation have been established for leak detection and emission quantification in
107 numerous cities (Fernandez et al., 2022; Defratyka et al., 2021; Luetschwager et al., 2021;
108 Keyes et al., 2020; Maazallahi et al., 2020; Ars et al., 2020; Weller et al., 2018; von Fischer et
109 al., 2017; Jackson et al., 2014). In-situ measurements of atmospheric CH₄ from mobile vehicles
110 are used to pinpoint and quantify CH₄ emission sources at street level in urban areas. The
111 mobile method was calibrated using above-ground controlled release experiments, in which
112 known amounts of CH₄ were released from gas cylinders (Weller et al., 2019). Simultaneous
113 measurements of carbon dioxide (CO₂) and ethane (C₂H₆) can provide valuable additional
114 information for attributing CH₄ sources (Maazallahi et al., 2020). A characteristic of the
115 resulting emissions distribution from gas distribution grids in cities is the existence of a few
116 leak locations with very high leak rates, up to 100 L min⁻¹, resulting in a right-skewed leak
117 emission rate distribution (Weller et al., 2020). Usually about 10% of the leaks are responsible
118 for between 30% to 70% of the emissions (Weller et al., 2019; Maazallahi et al., 2020).
119 Therefore, the CH₄ emission from the gas distribution system can be reduced very effectively
120 if the largest leaks can be found and fixed quickly, thus augmenting the routine leak detection
121 (carpet method) and repair programs with the mobile method.

122
123 The tracer dispersion method is another method to quantify CH₄ emissions from point and area
124 sources. In this method, a tracer gas is released at a known rate close to the outlet of the gas
125 leak, and both tracer and target gas concentrations are measured downwind. From these
126 measurements and the known tracer gas release rate, the target gas emission rate can be
127 determined with an uncertainty of ± 15% (Lamb et al., 1995) or less than 20% (Fredenslund et
128 al., 2019). Lamb et al. (2015) applied the tracer method to quantify leaks from urban
129 underground pipelines where they reported moderate agreement (± 50%) to excellent
130 agreement (± 5%) between the tracer and high-flow sampler method.

131
132 Another approach to quantify underground leak rates from buried gas pipelines is the so-called
133 suction method. In this method air is pumped out of the ground at a known rate via probes
134 surrounding the underground leaks until an equilibrium CH₄ mixing ratio is reached in air out-
135 flow, from which the CH₄ leak rate can be calculated. In Germany, this approach is applied to
136 a limited number of leak locations, which do not have to be repaired immediately or within 1
137 week. Suction measurements normally find leak rates that are < 2 L min⁻¹ (E.ON, personal
138 communication, 2020). The reported uncertainty range of this method is ± 10% based on 23
139 measurements in the 1990s (E.ON, personal communication, 2020). The discrepancy between
140 these rather low leak rates compared to leak rates inferred with the mobile method calls for
141 further investigation, since the suction method is also employed to derive network-wide
142 emission factors for the German country-wide gas distribution network (Federal Environment
143 Agency, 2020).

144
145 Hendrick et al. (2016) used surface flux chamber measurements carried out between 2012 and
146 2014 to estimate gas leak rates from 100 leak locations in the Boston area that were detected

147 using mobile measurements ($n = 45$) in 2011 from Phillips et al. (2013) and additional locations
148 from later mobile surveys ($n = 55$). They reported CH_4 emission rates from gas leaks ranging
149 from 0.003 g min^{-1} to 16 g min^{-1} , corresponding to roughly $0.0 - 24.4 \text{ L min}^{-1}$. They also
150 reported that their estimate using chamber measurements underestimated total CH_4 emissions,
151 likely because the chambers didn't capture the total CH_4 emitted from the leak. This is similar
152 to the enclosure measurements results from Weller et al. (2018).

153

154 The flow through a hole in a pipeline can also be calculated theoretically and empirically from
155 the physical properties of the hole, mainly the ratio of hole to pipeline diameter and the
156 overpressure in the pipeline. There are three different engineering model types to estimate
157 emissions from gas leaks: the hole model, the rupture model and modified models to bridge the
158 gap between hole and rupture models (Hu et al., 2020; Moloudi and Esfahani, 2014; Yuhua et
159 al., 2002; Arnaldos et al., 1998). These types of models are either to estimate leak strength from
160 a pipeline in open space or a buried pipeline. A leak on a buried pipeline has higher surrounding
161 resistance depending on soil conditions compared to a situation where the pipeline is in open
162 space. Such models have been used to quantify emissions from holes in pipelines in open space
163 (Hou et al., 2020; Manda and Morshed, 2017; Moloudi and Esfahani, 2014; Mahgerefteh, Oke
164 and Atti, 2005; Yuhua et al., 2003; Kayser and Shambaugh, 1991) but also from buried
165 pipelines (Liu et al., 2021; Ebrahimi-Moghadam et al., 2018; Okamoto and Gomi, 2011; Yan,
166 Dong and Li, 2015). Cho et al. (2021) introduced a model, which takes into account soil
167 properties including absolute and relative permeability and porosity, the underground spread
168 of the leak, surface CH_4 mole fractions and depth of the buried pipeline based on experiments
169 with a controlled release rate. This model was calibrated based on release rates ranging from
170 1.3 g min^{-1} to 5.7 g min^{-1} , corresponding to roughly $2.0 - 8.7 \text{ L min}^{-1}$.

171

172 In this study, we present results from measurements with the mobile, the tracer release and the
173 suction methods in Hamburg, Germany, in August and September 2020. We present the
174 quantitative emission estimates as well as a qualitative intercomparison of the three methods,
175 in particular related to the applicability and the strengths and weaknesses of the different
176 methods at different leak locations. We investigate differences between the leaks detected from
177 mobile measurements and leak locations reported from the routine leak detection surveys
178 performed by the local gas utility (hereinafter LDC (Local Distribution Company)). Finally,
179 we discuss implications of our study for national emission inventories.

180

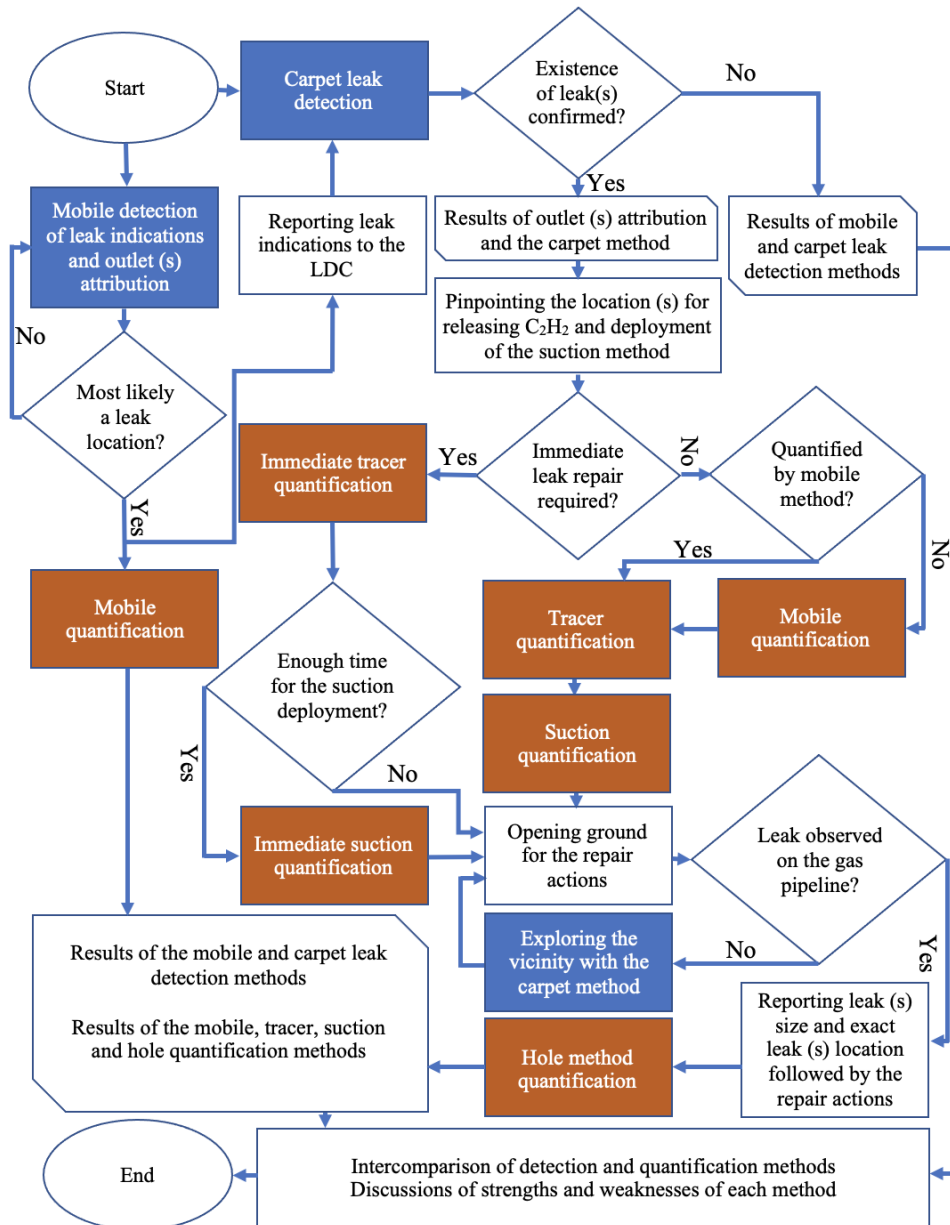
181 **2 Materials and Methods**

182 **2.1 Campaign preparation and general overview**

183 As a preparation for the intercomparison campaign, all partners contributed to the preparation
184 of an "intercomparison matrix" where the characteristics and deployment details of the
185 different methods were specified. This matrix is provided in section S.1 of the Supplemental
186 Information (SI). The matrix includes descriptions related to the identification of gas leaks, the
187 quantification of gas leaks, adjustments of the method to the intercomparison exercise and
188 upscaling. It also laid out an initial plan for the intercomparison in terms of identification of
189 suitable locations and deployment of the different methods.

190 According to this plan (Fig. 1), we first applied the mobile method to identify potential gas leak
191 locations, namely leak indications (LIs). When the mobile method had detected one or more
192 emission outlets (See Sect. S.2 in SI) and classified them as a potential gas leak location, the
193 carpet method was applied to confirm the leak and determine the confine leak location. Some
194 additional locations that had previously been identified by the carpet method (leak categories
195 B and C) were added to the list of target locations.

196 Following leak detection, the mobile quantification method (multiple transects) was applied on
 197 all the locations and the tracer and suction methods were applied at the confirmed leak
 198 locations, and with some restrictions regarding safety and method capacities. The release
 199 location for the tracer quantification method was confirmed based on surface screening using
 200 a handled methane analyzer. For comparison of the mobile and tracer release methods with the
 201 suction and hole methods we assumed that (i) a steady state between pipeline leakage under-
 202 ground CH₄ accumulation and emission to the atmosphere had been reached (Kirchgessner et
 203 al., 1997) and (ii) methanotrophs and methanogens have negligible impact on quantification of
 204 gas leak emissions. Thus, the total emission rate of all outlets in the vicinity of a leak location
 205 is equal to the natural gas emission rate from the pipeline leak. We will discuss implications of
 206 the above assumptions for selected cases. After leak repair, the LDC reported leak hole sizes,
 207 pipeline diameters and pipeline operational pressures, allowing leak rate estimation with the
 208 hole method.



209
 210 **Figure 1 – Flowchart of application of leak detection methods (blue colors) and**
 211 **quantification methods (red colors) followed by repair actions and intercomparison of**
 212 **the detection and quantification methods**

213 **2.2 Measurements setups**

214 **2.2.1 Mobile measurement setup**

215 Onboard the measurement vehicle (VW Transporter) we operated two cavity ring-down
216 spectrometers (CRDS), model G2301 and model G4302 (Picarro, Santa Clara, California,
217 USA). The G2301 measures CH₄, CO₂ and water vapor (H₂O) at a flow rate of $\approx 0.2 \text{ L min}^{-1}$
218 and 0.3 Hz frequency. The G4302 has a flow rate of $\approx 2.2 \text{ L min}^{-1}$ and sampling frequency of
219 about 1 Hz for CH₄, C₂H₆ and H₂O. The air intake for both instruments was from the same
220 tubing attached to the front bumper. This setup allowed us to directly compare the
221 enhancements observed from the two instruments during surveys. The G4302, which is in a
222 shape of a backpack, was also used in attribution of outlets emissions in walking surveys to
223 check presence of C₂H₆ in emission outlets.

224

225 **2.2.2 Tracer release measurement setup**

226 The tracer release method was applied by releasing acetylene (C₂H₂) at the emission outlet
227 identified by the mobile leak detection and confirmed by the carpet method. The tracer gas
228 was released at the main emission outlet, which was confirmed by surface screening using a
229 handheld CH₄ analyzer. Tracer release rates between 1.3 and 2.6 L min⁻¹ from a gas cylinder.
230 A Picarro CRDS, G2203 instrument was used to measure CH₄ and C₂H₂ mole fractions
231 continuously with $\approx 0.3 \text{ Hz}$ frequency. The instrument was installed in a measurement vehicle
232 (VW Caddy), and air was sampled from the atmosphere through an inlet on the roof about 2m
233 above ground. The tracer method was applied either in static mode, where air was sampled in
234 one or a few locations downwind from the outlets and tracer release locations ($n = 11$) or mobile
235 mode ($n = 5$), where the plumes were transected while measuring concentrations of CH₄ and
236 C₂H₂. The choice of mode depended on the site conditions including road accessibility and
237 wind direction. The tracer release setup including instrumentation used as well as mobile mode
238 is described in detail in Mønster et al (2014), and the principle of the static mode is described
239 in Fredenslund et al (2010).

240

241 **2.2.3 Suction measurement setup**

242 In the suction method, 12 probes were used to insert in the soil around the confirmed gas leak
243 location by the LDC. The probes are connected to a pump to extract accumulated subsurface
244 CH₄ from the leak. CH₄ mole fraction at the outflow is measured with a Flame Ionization
245 Detector (*MEEM*, 2018).

246

247 **2.2.4 Carpet method setup**

248 Leak detection experts from the LDC operate a methane detector (Sewerin instruments,
249 Gütersloh, Germany) on a rolling device, where a plastic cover (the carpet) moves over the
250 ground and provides a loose seal to the surrounding atmosphere, facilitating preferential
251 analysis of air emanating from the surface right below the carpet. The instrument gives an
252 acoustic signal when a high CH₄ from a potential leak has been detected. The instrument can
253 detect C₂H₆ with a gas chromatograph, which take about couple of minutes per outlet location.

254

255 **2.3 Detection, confirmation and attribution of emissions at gas leak locations**

256 **2.3.1 Mobile detection of possible leak location**

257 For leak detection with the mobile method, we first evaluated CH₄, C₂H₆ and CO₂ signals
258 during mobile surveys. If (i) CH₄ and C₂H₆ signals were observed with a ratio of less than 10%
259 with no CO₂ signal or (ii) CH₄ was observed ($< 500 \text{ ppb}$ enhancement on G4302) with no C₂H₆
260 and CO₂ signals, then we parked the mobile measurement car, detached the G4302 analyzer
261 from the system and searched for gas outlets on foot with the G4302. This detailed search for
262 outlets was performed to (i) confirm the presence of both CH₄ and C₂H₆ signals (ii) map the

263 spatial spread of outlets and (iii) spatially constrain the possible gas leak location. The reported
264 possible gas leak locations from the mobile method were then reported to the LDC for
265 confirmation and localization of the leak with the carpet method and subsequent underground
266 measurements.

267

268 **2.3.2 Attribution of leak indication signals from mobile measurements**

269 To attribute an observed leak indication (LI) from mobile measurements to a source category,
270 namely fossil, microbial and combustion, we used CO₂ and C₂H₆ signals, which were
271 continuously measured along with CH₄. We quantitatively evaluated C₂:C₁ ratios (%) when (i)
272 the CH₄ enhancements were larger than 0.5 ppm (ii) C₂H₆ enhancements were also larger than
273 15 ppb and (iii) the determination coefficient (R²) of the linear regression between CH₄ and
274 C₂H₆ was larger than 0.7. If CH₄ signals in mobile measurements were associated with CO₂
275 and high C₂H₆ mole fractions (C₂:C₁ > 10%), we attributed those emissions to combustion
276 (Maazallahi et al., 2020). When we repeatedly observed CH₄ enhancements, no CO₂
277 enhancements and C₂:C₁ ratios between 1 and 10%, or we observed persistent CH₄ signals in
278 several passes we did further on-foot inspection of the outlets. If the emissions from the outlets
279 clearly pointed to a fossil origin based on the CH₄ and C₂H₆ signals, we labeled the locations
280 as potential gas leak locations and reported them to the LDC for confirmation. We only
281 considered a location as a gas leak for further investigation if the LDC confirmed the existence
282 of a gas leak.

283 If at a particular location, we observed several CH₄ maxima, for example from different outlets,
284 we considered the “strongest” outlet as the main emission point. The “strongest” emission point
285 refers to a point where we observed the highest CH₄ mole fraction when the G4302 intake inlet
286 was put at a distance of ≈ 2 - 5 cm above the surface or outlet. When several emission outlets
287 with similar mole fractions were found, we considered the spatial average of the coordinates
288 as the main emission point. The tracer method then released C₂H₂ at the main outlet emission
289 point.

290 The LDC reported a C₂:C₁ ratio of 3.0% (96.20 ± 0.02 mol % CH₄ and 2.88 ± 0.00 mol %
291 C₂H₆, GNH personal communication) for the gas composition in the grid for the period of
292 August and September 2020 in Hamburg. This ratio was reported 3.5% (95.09 mol % CH₄ and
293 3.37 mol %, GNH personal communication) in April 2020.

294

295 **2.3.3 LDC leak detection and confirmation**

296 Since the pipeline locations are known to the LDC, the method can be applied precisely above
297 the pipelines, including visible cracks and cavity outlets in the close vicinity, increasing the
298 possibility of leak detection. Once the carpet method detects a CH₄ source, a second
299 measurement is performed above the location with the highest signal, where air is accumulated
300 and analyzed for the presence of C₂H₆. The C₂H₆ detection in the carpet method is not online
301 with higher detection threshold and in batch mode (gas chromatography), which takes time, 5
302 – 10 minutes per location. If sufficiently high CH₄ and C₂H₆ levels are found, the leak is
303 categorized in one of safety categories of A1, A2, B or C.

304

305 **2.3.4 Precise underground leak localization**

306 When a leak has been confirmed with the carpet method, a precise localization of the leak is
307 performed by drilling holes about 20-40 cm into the ground along the pipeline track and
308 measuring the sub-surface CH₄ concentration. The location with the maximum sub-surface
309 reading is assigned the most likely leak location where the repair teams open the road and
310 attempt repair of the leak. The final exact leak location is reported after opening ground for the
311 repair reactions. Mostly the locations reported from the carpet method matches the locations

312 reported from the leak repair team, which depends on the transport pathways of emission
313 undersurface and surface coverage.

314

315 **2.4 Emission quantification**

316 **2.4.1 Mobile measurements quantifications**

317 After the detection of the target locations, we performed additional transects at these locations
318 on different days. We accepted a mobile measurement transect of a leak location for further
319 analysis if (i) the GPS signals of transects were logged correctly along the street track and (ii)
320 at least one of the two instruments, G2301 (for quantification and attribution) and / or G4302
321 (for attribution), were running during the transect and (iii) the transect track included at least
322 one GPS coordinate less than 50 m from the leak location. The start and end point of the
323 accepted transects were determined as the locations where the driving tracks intersected with a
324 circle with radius of 100 m centered at the gas leak location reported by the LDC, or a reported
325 outlet location from the mobile method, for the locations where the LDC did not confirm a
326 leak. The segments between the start and end points were evaluated one by one (See an example
327 in Sect. S.4.1 in SI) to determine various parameters, e.g., the maximum CH₄ enhancements,
328 plume area, driving speed, distance to the actual leak locations, etc. The plume area is the
329 integral of the CH₄ enhancements above background along the driving track from the location
330 where the CH₄ enhancement exceeds > 10 ppb until the location where it falls again below the
331 10 ppb threshold.

332 Gas leak quantification from mobile measurements is based on an empirical equation derived
333 from controlled release experiments reported by von Fischer et al., (2017) and reevaluated in
334 Weller et al., (2019) (Eq. 1).

335

$$336 \quad Q = \exp \left(\overline{\ln (C_{max})} + 0.988 \right) / 0.817 \quad \text{Eq. 1}$$

337

338 In Eq. 1, C_{max} is the maximum CH₄ enhancement (ppm) observed during each transect next to
339 the leak location. The maximum CH₄ enhancement should be more than 10% above CH₄
340 background level to be considered for the quantification algorithm. The emission rate is
341 denoted by Q and it is in L min⁻¹. $\overline{\ln (C_{max})}$ is the mean of the logarithm of the maximum
342 mole fraction enhancements for all accepted transects.

343 The standard quantification method only uses transects where CH₄ enhancements are more
344 than 10% or ≈ 200 ppb above background level. This 10% enhancement threshold corresponds
345 to about 0.5 L min⁻¹ emission rate in Eq. 1. Thus, ≈ 0.5 L min⁻¹ is the minimum emission rate
346 that can be quantified with Eq. 1 and leaks with smaller emission rates are ignored by design
347 of the method. Below we investigate the effect of relaxing the enhancement threshold. The
348 application of the tracer release technique in mobile mode allowed us to use the known C₂H₂
349 release rate and the measured C₂H₂ plumes to independently validate the mobile approach,
350 including the effect of the enhancement threshold. We also investigated the effect of distance
351 between CH₄ maxima to gas leak locations, which is not a parameter in Eq. 1.

352 The uncertainty of the emission rate for each location in the mobile method was calculated
353 using standard error and t-factor (95% confidence) for the locations with at least three CH₄
354 enhancements greater than the 10% threshold.

355 In addition to evaluating the maximum CH₄ enhancement from each transect we also derived
356 the plume area (mixing ratio times distance and in unit of ppm m) for comparison between the
357 instruments. In principle, the plume area should provide a more robust quantification of an
358 ambient CH₄ plume than the maximum enhancement: When a plume spreads out, individual
359 realizations of the plume can be sharper and higher, or wider and lower, depending on
360 meteorological conditions, but the plume area should be less affected. In addition, when an
361 instantaneous plume is sampled with two instruments with different gas flow rates, instruments

362 with a lower flow rate will be affected by mixing of air in the measurement cell. This will lead
 363 to a lower maximum enhancement but a wider peak, and thus the peak area should lead to a
 364 better comparison between the instruments.

365

366 **2.4.2 Tracer measurements quantifications**

367 The tracer method uses Eq. 2a to quantify CH₄ emissions in mobile mode (integral over space
 368 dimension) and Eq. 2b in the static mode (integral over time dimension). Parameters relevant
 369 for the evaluation with the tracer method are provided in Sect. S.4.2.

$$370 \quad Q_{CH_4} = Q_{C_2H_2} \cdot \frac{\int_{start}^{end} C_{CH_4} dx}{\int_{start}^{end} C_{C_2H_2} dx} \cdot \frac{MW_{CH_4}}{MW_{C_2H_2}} \quad \text{Eq. 2a}$$

$$371 \quad Q_{CH_4} = Q_{C_2H_2} \cdot \frac{\int_{start}^{end} C_{CH_4} dt}{\int_{start}^{end} C_{C_2H_2} dt} \cdot \frac{MW_{CH_4}}{MW_{C_2H_2}} \quad \text{Eq. 2b}$$

372

373 Here C is the mole fraction (ppm) and MW is the molecular weight of the species, 16 g mol⁻¹
 374 for CH₄ and 26 g mol⁻¹ for C₂H₂. Q_{CH_4} is the CH₄ emission rate estimate for CH₄ (g s⁻¹) and
 375 $Q_{C_2H_2}$ is the controlled release rate of C₂H₂ (g s⁻¹). The C₂H₂ flow rate was controlled and
 376 measured with a flow controller (Brooks Sho-Rate). In addition, the mass of C₂H₂ released at
 377 each location was measured by weighing the release cylinder before and after the tracer release
 378 with a precise scale (KERN DE60K5A). The change in mass was then converted to a mass
 379 flow rate using the release time. To convert the emission rate from mass (g s⁻¹) to volume (L
 380 min⁻¹) we used normal temperature and pressure (NTP) conditions, T = 293.15 K, p = 1.01325
 381 bar. The locations of tracer release (C₂H₂) at the confirmed gas locations were determined with
 382 the combined information from the mobile and the carpet methods.

383 The tracer gas can also be used to pinpoint and confirm the emission source location. Prior to
 384 quantification, it is important that the emission outlet is located for proper tracer release (see
 385 Fig. 1) and source simulation and that other potential interfering emission sources can be ruled
 386 out. This is secured by performance of upwind and downwind CH₄ mole fraction screening.
 387 During transecting of the CH₄ and tracer plumes, the two plumes should match, if this is not
 388 the case, the tracer release should be relocated until a proper plume match is obtained. If an
 389 emission source consists of multiple outlets, the combined emission from all outlets can be
 390 measured by releasing the tracer at the main outlet and increasing the measuring distance until
 391 one confined overlapping plume of CH₄ and tracer gas is obtained. If the distance cannot be
 392 increased to access limitations, tracer should be released at each single emission outlet.

393

394 **2.4.3 Suction measurements quantifications**

395 The quantification of a leak with suction method is possible after pumping accumulated air out
 396 of soil and reaching CH₄ mole fraction equilibrium in the outflow. With the equilibrium CH₄
 397 reached and the known pumping rate through the probes, it is then possible to calculate
 398 emission rate (See Sect. S.4.3 in SI).

399

400 **2.4.4 Hole method, based on leak and pipeline properties**

401 The LDC reported the physical properties of gas leaks and pipeline conditions. These include
 402 leak area, pipeline diameter and pipeline operational pressure. In order to get an estimate of the
 403 upper physical limits of gas leakage through a hole with the given properties, we used the
 404 empirical model by Liu et al., (2021), which was designed to quantify emissions from buried
 405 natural gas pipelines to estimate emission rates from the leaks (Eq. 3), hereinafter “hole”
 406 method.

407

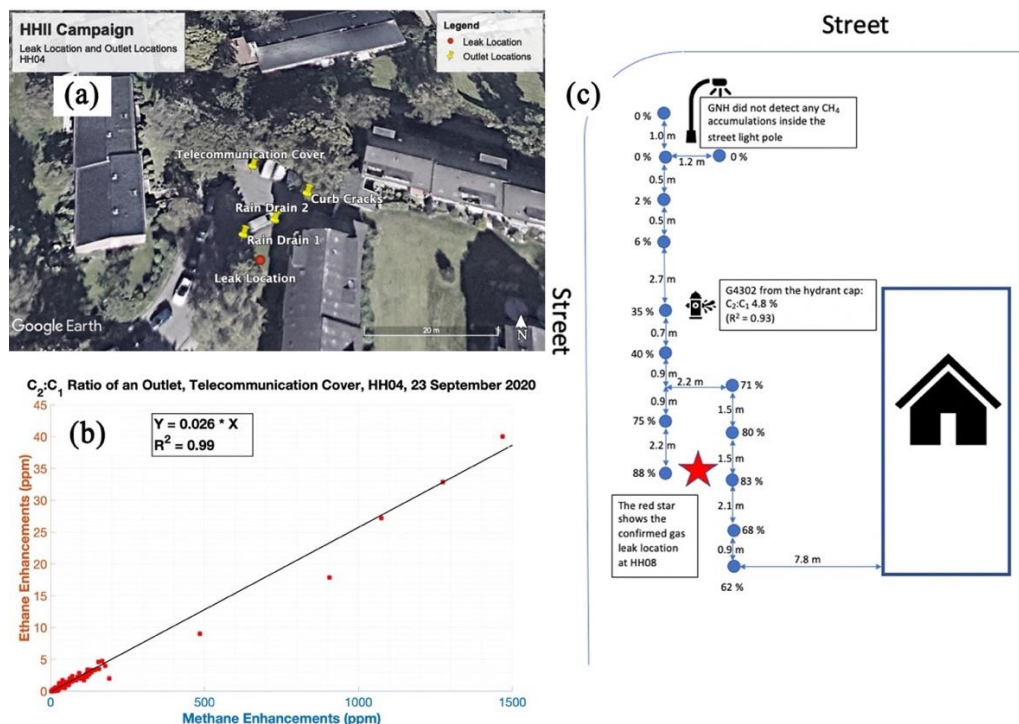
408 $Q = 0.567 \cdot [(h + 139.592)^{-0.1} - 0.542] \cdot d^{1.5} \cdot p^{0.7}$ Eq. 3
 409

410 Here, Q is the gas leak rate in $\text{m}^3 \text{h}^{-1}$ (at standard atmospheric conditions and converted to
 411 NTP), h is the depth of the buried pipeline in cm, d is the gas leak hole diameter in mm and p
 412 is the pipeline overpressure in kPa. We used 150 cm as pipeline depth for all the locations in
 413 Hamburg to estimate emission rate. We note that the model that we employed is for buried
 414 pipelines not pipelines in open space, and emission estimates for the gas leak emission rate in
 415 open space would be even higher (See Sect. 4.4 in SI). Ebrahimi-Moghadam et al. (2018)
 416 showed that CH_4 emission from a pipeline hole area can be between 7 to 10 times higher in
 417 open space relative to the subsurface conditions.
 418

419 3 Results

420 3.1 Leak Detection

421 15 possible leak locations were detected by the mobile method in the initial surveys, (labeled
 422 as HH001 – HH015). At 13 out of these 15 locations, leaks were confirmed by the LDC, HH007
 423 and HH012 locations were not confirmed as gas leak locations. In addition, the LDC identified
 424 5 other leak locations (labeled as HH100 – HH104) that had not yet been fixed (category B and
 425 C). The overview of the measurements (detection and quantification) is provided in the SI (See
 426 Sect. S.5 in SI). At some locations we also observed that vegetation was impacted negatively
 427 by the presence of leaks in their vicinities, a known phenomenon as high levels of methane
 428 cause harmful anoxic conditions for the plant roots (See Sect. S.6 in SI). At several locations
 429 the outlet identification was straightforward, because we only observed one outlet, but at 5
 430 locations we observed numerous outlets spread over a large area. Figure 2 shows the spread of
 431 emission outlets at one of the locations (Fig. 2a), with correlations of CH_4 and C_2H_6 at the
 432 “strongest” outlet (Fig 2b). Fig. 2c shows precise gas leak location practice of the LDC at one
 433 of the other locations.
 434



435 **Figure 2 – (a) aerial image of location HH004 (© Google Maps). Yellow pins show surface**
 436 **emission outlet locations, and the red point shows the actual pipeline leak location**
 437

438 reported by the LDC; (b) correlation between CH₄ and C₂H₆ measured from a
 439 telecommunication cover; (c) Map (not to scale) of drilled holes (blue dots) to locate the
 440 pipeline gas leak at HH008. The red star shows the actual pipeline gas leak location as
 441 indicated by the undersurface CH₄ mole fractions (See Sect. S.3, Fig. S3)
 442

443 3.2 Leak Quantification

444 Table 1 shows the results of the leak emission rate quantifications from the four methods. All
 445 these locations were quantified by the mobile method, although for 6 of them the 10%
 446 enhancement threshold was not reached. 16 locations were quantified by the tracer release
 447 method and 8 by the suction method. A complete overview of key parameters for all
 448 measurements (detection and quantification) is provided in Sect. S.5.
 449

450 Table 1 – Results of gas leak quantification with different methods in Hamburg, Germany

	ID	Leak quantification methods (L min ⁻¹)						Info. from the LDC				
		Mobile (measurements from G2301)			Tracer (L min ⁻¹)	Suction		Hole (L min ⁻¹)	Pipeline buried year	Leak size (cm ²)	Leak type; Safety considerations	Pipeline Size and Material#
		Transect (s) w/ CH ₄ Enh. > 10% threshold	Emission average	Emission range; 95% confidence		Emission (L min ⁻¹)	Status					
Detected by mobile method	HH001	n = 1 (10%)	0.7	-	0.06	<1.8	INC	39	1935	2.5	C	DN80ST
	HH002	n = 5 (50%)	4.9	0.7 – 36.0	0.22	<0.7	INC	45	1935	3.0	A2	DN80ST
	HH003	n = 6 (86%)	7.5	1.1 – 53.0	1.37	-	-	-	1963	-	A1	DN100ST
	HH004	n = 4 (100%)	7.8	1.8 – 34.5	5.33	-	-	-	1959	-	A1	DN80ST
	HH005 ⁺	n = 19 (51%)	1.8	0.9 – 3.6	0.21	-	-	-	1935	-	A2	DN80ST
	HH006 [*]	n = 11 (39%)	1.2	0.8 – 1.8	0.02	0.3	CPLT	33	1934	0.5	B	DN80ST
	HH007 [°]	n = 0 (0%)	-	-	-	-	-	-	-	-	-	-
	HH008	n = 6 (26%)	1.5	0.4 – 6.4	0.32	<1.3	INC	-	1934	-	C	DN80ST
	HH009 [×]	n = 9 (38%)	3.9	1.5 – 9.8	4.86	<3	INC	-	1928	-	A1	DN80ST
	HH010	n = 3 (38%)	1.6	0.2 – 13.7	0.51	<0.7	INC	-	1937	-	C	DN200ST
	HH011 [^] ×	n = 4 (50%)	1.9	0.2 – 18.6	0.37	-	-	150	1963	15	A1	DN300ST
	HH012 [°]	n = 0 (0%)	-	-	-	-	-	-	-	-	-	-
	HH013 [^]	n = 2 (40%)	1.8	-	-	-	-	65	1939	5	A1	DN80ST
	HH014	n = 24 (55%)	1.6	1.1 – 2.5	1.41	-	-	65	1950	5	A1	DN100ST
	HH015	n = 1 (50%)	1.0	-	0.38	<0.9	INC	19	1935	1	A1	DN80ST
Reported by the LDC	HH100	n = 1 (13%)	0.7	-	0.14	-	-	-	1994	-	C	d225Pe
	HH101	n = 0 (0%)	-	-	0.07	<0.7	INC	-	1960	-	C	DN80ST
	HH102	n = 0 (0%)	-	-	0.01	-	-	-	1928	-	C	DN125ST
	HH103	n = 0 (0%)	-	-	0.03	-	-	-	1963	-	B	DN150ST
	HH104	n = 0 (0%)	-	-	-	-	-	-	1930	-	C	DN100ST

451 ⁺ The LDC reported three leak locations, ≈ 30 m distance between the two ends, for this
 452 location: two leaks with area of 5 cm² and one leak with area of 1 cm²

453 ^{*} Complete measurements for the suction method and used for averaging

454 [^] Leak size reported as sum of total hole area of all the leaks on the pipeline

455 [×] Large difference between leak location and the tracer release location

456 [°] The LDC did not confirm a gas leak

457
458
459

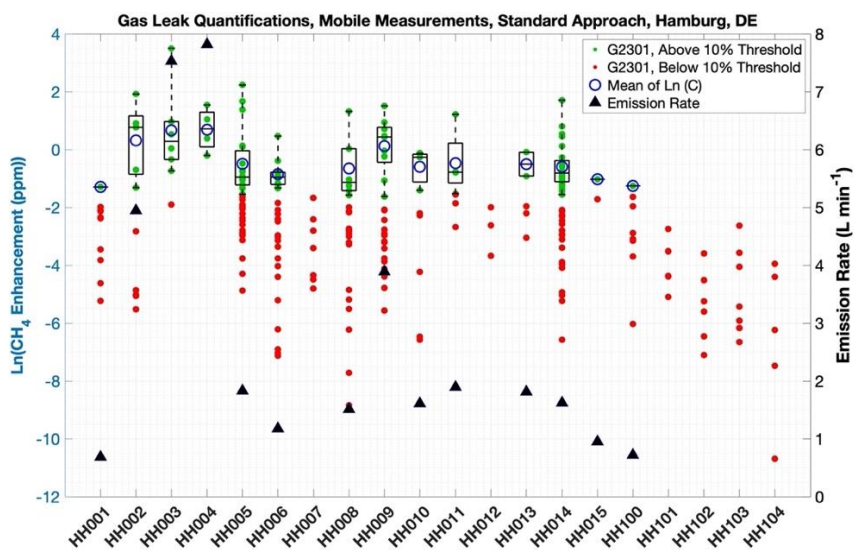
Pipeline materials, steel (ST) or Polyethylene (Pe), pipeline Diameter Nominal (DN), which is close to the inner pipeline diameter in mm

3.2.1 Mobile method

461 The mobile method was applied at all the 20 locations (18 confirmed and 2 unconfirmed gas
462 leak locations). At 14 (all confirmed gas leak locations) out of the 20 locations, CH₄
463 enhancements above the 10% threshold were observed and could be evaluated with the
464 standard algorithm. The emission rate estimates for these 14 gas leak locations ranged from 0.7
465 to 7.8 L min⁻¹. At the 6 other locations we didn't observe any CH₄ enhancements above the
466 10% threshold. When we lowered the enhancement threshold to 10 ppb, the emission rates
467 were 0.07 (HH007; not confirmed gas leak location), 0.1 (HH012; not confirmed gas leak
468 location), 0.04 (HH101), 0.02 (HH102), 0.05 (HH103) and 0.02 L min⁻¹ (HH104). Of the 5
469 leak locations reported by the LDC, 4 did not show any enhancement maximum above the 10%
470 threshold, i.e., these locations would not have been identified with the default algorithm
471 (Weller et al., 2018) and would thus not produce an emission estimate.

472 Fig. 2 shows a summary of all individual observed enhancement maxima with the G2301
473 analyzer from all transects with the mobile vehicle, which were used for the quantification of
474 emission rates with Eq. 1. The figure illustrates the large spread in enhancement maxima for
475 multiple passes at each location, similar to Luetschwager et al (2019), leading to large
476 uncertainties in emission estimates of individual locations. Fig. 2 also shows the diversity of
477 the various locations, where at some locations most or all of the observed enhancement maxima
478 are above the 10% threshold (e.g. HH003 and HH004), at several locations none of the
479 enhancement maxima was above the threshold (e.g. HH101 and HH104) and at other locations
480 many transects showed enhancement maxima both above and below the threshold (e.g. HH006,
481 HH008, HH009, HH014).

482 As shown in Fig. 3, there is a wide range of CH₄ enhancement observations per location. This
483 depends on wind conditions, distance of the observed plume maximum to the emission outlet
484 location, the superposition of emissions from several outlets and likely other variables such as
485 soil water content. The mean relative uncertainty from the mean emission rate values for the
486 mobile method is ≈ 70% for lower and 400% for the upper ends for the locations with at least
487 3 transects (n = 10) which pass the 10% enhancement threshold (significant signals) in this
488 study. The lower and upper ranges go down to 60% and 275% for the locations with at least 5
489 transects (n = 7) with significant CH₄ enhancements.



490
491
492

Figure 3 – CH₄ enhancement maxima from all individual transects for each location using G2301. Red points show CH₄ enhancement maxima below the 10% threshold, green

493 **points show CH₄ enhancement maxima above the 10% threshold, thus used for the**
494 **standard quantification. Blue circles show the $\ln(C_{max})$ of all the green points for each**
495 **location, and black triangles show the derived mean emission rate (based on all green**
496 **points) using Eq. 1 for the location with at least one green point (right y-axis).**

497

498 **3.2.2 Tracer method**

499 The tracer method performed emission rate quantification at 16 gas locations out of 20
500 locations. The derived emission rates range from 0.03 to 5.3 L min⁻¹ (Table 1). For 4 locations
501 the tracer method was not applied because (i) the emissions were not persistently observable
502 and the LDC also didn't confirm existence of gas leaks at these locations (n = 2; HH007 and
503 HH012) or (ii) the leak had already been repaired (n = 1; HH013) or (iii) no emission was
504 detectable during the visit of the tracer team (n = 1; HH104). For two of the locations (HH11
505 and HH09), where leaks were confirmed and the tracer method was successfully deployed,
506 later investigations during repair actions (see Fig. 1) showed that the surface emission outlets
507 were located far (15 to 60 m) from the actual gas pipeline leak location indicating underground
508 gas migration. It is evident from Table 2 that the tracer technique can also quantify very small
509 emission rates, below the cut-off of the mobile technique of 0.5 L min⁻¹. Emission rate
510 estimates derived from the tracer technique were in general lower than the ones derived from
511 the mobile technique, except for three sites where they were comparable (HH004, HH009 and
512 H014).

513

514 **3.2.3 Suction method**

515 Due to the time-consuming nature of the suction measurements, initially 10 gas leak locations
516 had been planned for deployment of the suction method in this campaign. The goal was to
517 cover a wide range of expected emission rates, as stated in the intercomparison matrix. The
518 suction method was applied at 8 gas leak locations (see Table 1) out of which the suction
519 quantification was complete (HH006) according to protocol where an equilibrium
520 concentration has to be reached. This was at HH006, with a derived emission rate of 0.3 L min⁻¹.
521 At several of the locations where the mobile method had indicated high emission rates,
522 subsurface accumulation was widespread, and the suction method was either not deployed (n
523 = 3; HH003, HH04, HH011) or the measurements were incomplete (n = 7; HH001, HH002,
524 HH008, HH009, HH010, HH015 and HH101) because of either safety reasons or because the
525 suction team estimated that they would be unable to complete the measurements within a day.
526 For the 7 locations with incomplete suction measurements, the emission rates were reported
527 ranging from 0.7 to 3 L min⁻¹. These can be regarded as upper limit estimates because suction
528 was not yet completed and CH₄ concentrations would have supposedly dropped further.

529

530 **3.2.4 Hole method**

531 For 5 locations where the leak area of a single gas pipeline leak was reported, the corresponding
532 emission rates are between 19 to 65 L min⁻¹. For locations HH011 and HH013, the hole area
533 was reported as the sum of several holes and the total hole area for these two locations resulted
534 in an emission rate of 150 and 65 L min⁻¹, respectively. The quantification from the hole method
535 is higher than from the mobile, tracer and suction methods by at least an order of magnitude.

536

537 **3.3 Leak categories**

538 The 20 (18 confirmed + 2 not confirmed) locations can be divided into four main categories
539 related to measurement challenges of the various methods. These categories may overlap.

- 540 (i) Large subsurface CH₄ accumulation
- 541 (ii) Insufficient CH₄ enhancements for mobile quantification
- 542 (iii) Large CH₄ enhancement variability for mobile quantification

543 (iv) Several outlets and / or leaks or atmospheric turbulence

544 In this section we present the overall results and discuss in detail one selected location for each
545 of these categories. The remaining locations (with similar characteristics) are presented in the
546 SI.

547

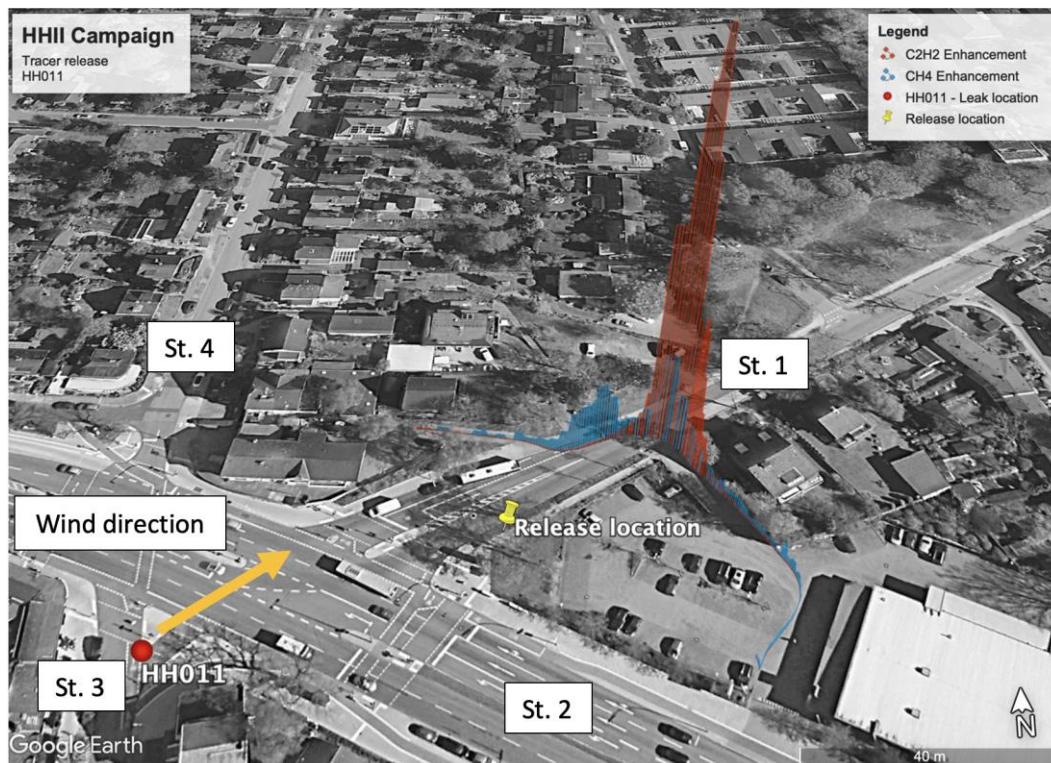
548 **3.3.1 Location type I – Large subsurface CH₄ accumulation and multiple outlets**

549 The spatial spread of surface emission outlet locations identified with the G4302 instrument as
550 part of the mobile method provides an indicator for the extent of the subsurface accumulation
551 of CH₄. For 5 locations, emission outlets were found at great distance from each other, in order
552 of tens of meters. The total emission of a gas leak is equal to the sum of emissions from all the
553 surface outlets at a location, thus it is necessary to quantify each outlet separately to get the
554 total emission.

555 HH011 (Fig. 4) is an example where very widespread CH₄ accumulation and migration was
556 observed. During the initial mobile gas leak detection, leaks were located at the intersection of
557 streets 1 and 2, close to a subsurface vent and a rain drain, ≈ 2 m far apart, (the yellow pin in
558 Fig. 4a) based on clear signals from these outlets and a sign next to the road indicating presence
559 of gas pipelines. The vent showed a C₂:C₁ ratio of 2% (R² of 0.8 and max CH₄ mole fraction
560 of 31 ppm) and we observed C₂:C₁ ratio of 2.8% with R² of 0.96 and max CH₄ mole fraction
561 of ≈ 70 ppm from the rain drain, clearly indicating a large / dominant contribution from fossil
562 CH₄. However, after quantifying the emission from these two leaks using the mobile and the
563 tracer release methods, the LDC found the actual gas pipeline leak, during the repair actions,
564 on the south side of the intersection, far from the vent and the rain drain, at the intersection of
565 street no. 3 and no. 2 indicating that the gas had travelled about 60 m underground. It is possible
566 that the leak resulted in several gas emission outlets, likely closer to the gas pipeline leak
567 location. The emission rate measured using the mobile method was 1.6 L min⁻¹ based on 5
568 plume transects and is likely underestimated because some emission outlets potentially were
569 not included in the performed plume transect. It should also be noted that the distance from the
570 gas pipeline leak location to the plume transect is larger than the distances applied during the
571 controlled release calibrations (average 15 m) (Weller et al., 2019).

572 The tracer was released at the vent and the rain drain and thus measured the combined emission
573 from these two outlets to be 0.4 L min⁻¹. If the gas pipeline leak gave rise to multiple
574 unidentified surface emission outlets, the emission from the gas pipeline is underestimated. IN
575 fact, Fig. 4b shows that a CH₄ plume without C₂H₂ was observed during the tracer release
576 measurements at HH011, confirming that at least one other source of methane emission was
577 present nearby.

578 Based on the previous experience at locations with widespread subsurface accumulation it was
579 concluded that the suction method could not be applied at this location. The other case in this
580 category was HH009.



581
 582 **Figure 4 – aerial image of HH011 (© Google Maps). A gas leak location with widespread**
 583 **undersurface CH₄ accumulation. The yellow pin shows the assumed leak location and**
 584 **location of tracer release, which was very different from the actual leak location as**
 585 **identified by the LDC (red circle). St. 1-4 are added to identify streets that are discussed**
 586 **in the text. General wind direction during tracer release deployment is shown with an**
 587 **orange arrow. CH₄ (in blue) and C₂H₂ (in red) levels measured at a plume transect. One**
 588 **of the CH₄ plume is proportional to the C₂H₂ plume while the other CH₄ plume lacks the**
 589 **C₂H₂ signals suggesting existence of at least another emission outlet.**

590
 591 The LDC reported the total area of several holes in the pipeline as 15 cm² for HH011, which is
 592 the largest leak size among all the locations. If we assume that there was one hole with this
 593 size, then the emission rate estimated by Eq. 3 will be 150 L min⁻¹, a hole of 5 cm² gives
 594 emission rate of 65 L min⁻¹. The pipeline for this location was DN300ST and has been in
 595 operation since 1963.

596
 597 **3.3.2 Location type II – Insufficient CH₄ enhancements for mobile quantification**

598 At HH101, on a narrow (≈ 3 m wide) street, which had about 1 m wide bare soil pavement on
 599 one side, the LDC reported a gas leak location based on their routine surveys. On both sides of
 600 the street there were about ≈ 1.5 m tall bushes and some trees. All three methods (mobile, tracer
 601 and suction method) were deployed at this location. Gas emissions found their way to the
 602 atmosphere through cracks in the asphalt with C₂:C₁ ratio of 2.5% (R² of 0.93) with max CH₄
 603 mole fraction of ≈ 25 ppm. None of the CH₄ enhancement maxima observed during the mobile
 604 surveys at this location were above the 10% enhancement threshold with the G2301 instrument,
 605 thus this location would not be labeled as LI and no quantification would be reported from
 606 mobile method as implemented in Weller et al (2019) and Maazallahi et al. (2020). The tracer
 607 method was applied in static mode at a distance of ≈ 15 m and reported an emission rate of 0.1
 608 L min⁻¹, which is compatible with the emission strength being below the “detection limit”
 609 defined by the 10% cut-off of the standard algorithm (0.5 L min⁻¹). When the emission strength
 610 is evaluated using the CH₄ enhancements below the cut-off, the value is 0.04 L min⁻¹. The

611 suction method was applied at this location but an equilibrium was not achieved after 9 hr, i.e.
612 incomplete suction measurements, and an upper limit for the emission rate of $\approx 0.7 \text{ L min}^{-1}$ was
613 reported. The fact that the suction measurement was incomplete at this location with a small
614 emission rate shows that subsurface accumulation can also be large for smaller leaks.

615 Three of the leak locations in this study only showed one CH_4 enhancement above threshold.
616 The 10% threshold is a constraint, which removes enhancements less than about 200 ppb. This
617 means for the locations where we only have one transect with CH_4 enhancements more than
618 the 10% threshold, the minimum emission rate estimated is about 0.5 L min^{-1} , no matter how
619 many transects we had with CH_4 enhancements less than the 10% threshold. This situation was
620 observed for HH001, HH015 and HH100 (Fig. 5). In this case, the mobile method likely
621 overestimates the total leak rate, because only the maximum enhancement is used for
622 quantification. The tracer method reported low emission rates for these three sites 0.12 L min^{-1}
623 on average ($n = 6$).

624 For the two locations (HH007 and HH012) where the LDC didn't confirm gas leaks (despite
625 periodic observation of C_2H_6 at outlets during the mobile surveys) none of the transects showed
626 CH_4 enhancement maxima above the 10% threshold. At HH007, the outlet was through cracks
627 in the pavement but at HH012 the outlets were from manholes. At HH007 the outlet location
628 had shifted by about 2 m for two different days (4-week gap). We note that the correlation
629 coefficients between CH_4 and C_2H_6 at these locations were between 0.4 and 0.6, so less than
630 0.7, which is the threshold correlation we accepted for the outlets. As a leak was not confirmed
631 for these locations, the tracer and suction methods were not applied.

632

633 **3.3.3 Location type III – Large CH_4 enhancement variability for mobile quantification**

634 For several locations, we observed a large variability of CH_4 enhancements from different
635 transects. One example is HH008, where only 6 of the 23 transects exceeded the 10% threshold,
636 i.e. the leak was only observed in about every 4th transect. The leak location of HH008 is an
637 example where CH_4 enhancements from several transects cover a wide range. Based on the 6
638 transects, which showed enhancement maxima above the 10% threshold, a leak rate of 1.5 L
639 min^{-1} is derived. This may be an overestimate since many transects with maxima below the
640 threshold were not considered. For this location the mobile tracer method was applied, which
641 resulted in a leak rate quantification of 0.3 L min^{-1} .

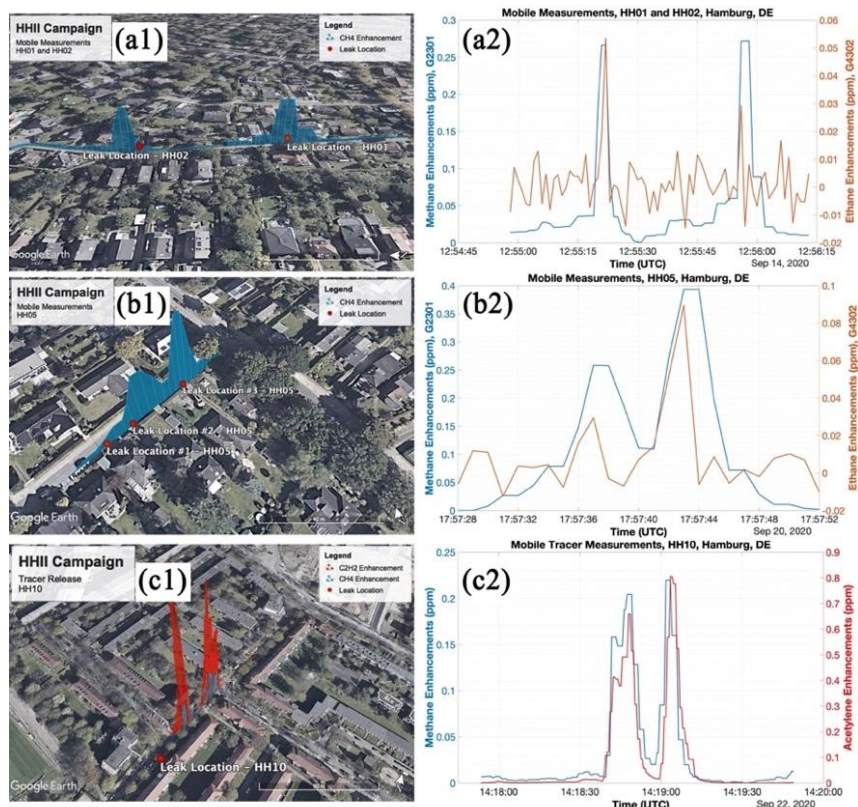
642 The suction method derived an upper emission estimate of 1.3 L min^{-1} from incomplete
643 measurements at HH008. The LDC reported a C category leak for this location from a DN80ST
644 pipeline, which was installed in 1934.

645

646 **3.3.4 Location type IV – Several outlets and / or leaks or atmospheric turbulence**

647 On a $\approx 5 \text{ m}$ wide street, we detected two leaks about 80 m away from each other, HH001 and
648 HH002 (Fig. 5a). It was a cobblestone street and there were bushes and few trees planted,
649 mostly on one side of the street. The mobile method performed 10 transects at both locations
650 and all the transects were accepted for the evaluation. The tracer team could quantify both
651 locations using static measurements. The suction team began to quantify HH002 and HH001,
652 but during quantification of HH001, there was a small accident (fire due to contact of drilling
653 head with electric cable) and the leak had to be fixed immediately. The plumes on this street
654 were sufficiently separated to positively identify two different leaks on the same street. In
655 contrast, at location HH005, we observed several maxima for the same transect, but because
656 the maxima were close to each other, those were clustered together in the mobile measurement
657 algorithm (Fig. 5b). Later the LDC reported even three individual pipeline leaks on this street.
658 In another example (HH010), some transects showed several plume maxima although only one
659 emission outlet and later on only one gas pipeline leak was found (Fig. 5c). However, the
660 release of the tracer resulted in several matching CH_4 and tracer gas plumes confirming that

661 the emission indeed occurred from a single outlet and that the multiple plumes at this location
 662 were due to inhomogeneous plume dispersion. This illustrates that the existence of several
 663 maxima in one transect does not necessary correspond to presence of several leaks and/or
 664 outlets, but it can also be related to a spatially heterogeneous/disturbed plume. This shows that
 665 the signals from the mobile detection method are not sufficient to allow determining the
 666 number of leaks at a location with several plume at a close distance from each other in a single
 667 transect.
 668



669 **Figure 5 - several maxima observed during a single transect on one street showing**
 670 **different situations: two well isolated leaks with about 80 m distance from each other (a1**
 671 **and a2, HH001 and HH002), three pipeline leaks close to each other with several**
 672 **outlets (b1 and b2, HH005) and one leak and one outlet but several CH₄ enhancement**
 673 **maxima due to turbulence (c1 and c2, HH10), aerial images: © Google Maps.**
 674
 675

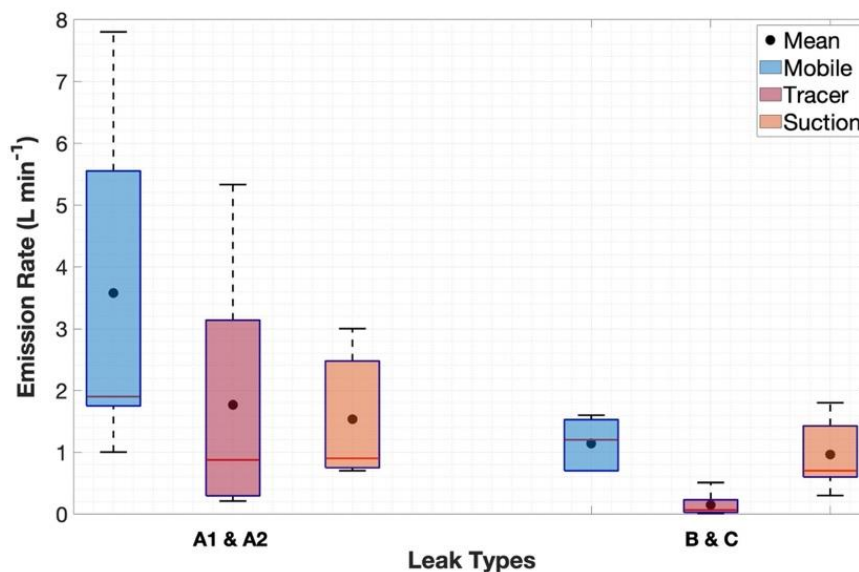
676 After detection by mobile measurements, emissions out of the ground were detected at HH001
 677 and HH002 with the G4302 backpack within 3 m distance from the gas pipeline leak locations,
 678 which was later reported by the LDC. For the single transect with a maximum above the 10%
 679 threshold observed with the mobile method, the derived emission rate at HH001 was 0.8 L min⁻¹
 680 (n = 1). For HH002, the derived emission estimate for the transects with maxima above the
 681 threshold is 5.2 L min⁻¹ (n = 5) from the mobile method. At HH002, individual derivation of
 682 emission from separate CH₄ enhancement gives a wide range between 0.7 and 36.0 L min⁻¹
 683 (95% confidence) from the mobile method (see category III above). For HH001, the tracer
 684 method was applied in static mode at ≈ 30 m distance to the release point and ≈ 40 m far from
 685 HH002. The derived emission rate for HH001 is 0.06 L min⁻¹ and for HH002 0.22 L min⁻¹ from
 686 the tracer method. For HH001, after about 5 hr of pumping, the suction quantification had to
 687 be stopped due to the incident described above. Based on the incomplete suction measurement
 688 an upper limit for emission rate of ≈ 1.8 L min⁻¹ for HH01 was estimated. An emission estimate
 689 of ≈ 0.7 L min⁻¹ was derived for HH002 from an incomplete suction measurement. The LDC

690 reported leak size of $\approx 2.5 \text{ cm}^2$ for HH001 and for $\approx 3 \text{ cm}^2$ for HH002 which then give emission
 691 rate of 39 and 45 L min^{-1} respectively from the hole method. For both locations, leaks were due
 692 to pipeline corrosion.

693

694 3.4 Emission rates of different leak safety types

695 The 18 confirmed gas leak locations that were investigated in the campaign were categorized
 696 into the four safety categories, A1 ($n = 7$), A2 ($n = 2$), B ($n = 2$) and C ($n = 7$). The mobile
 697 method quantified all the A1 and A2 leaks ($n = 9$) with an average emission rate of 3.6 L min^{-1} .
 698 5 out of 9 leaks in categories of B and C leaks were quantified with the mobile technique
 699 including the 10% threshold with average emission rate of 1.1 L min^{-1} ($n = 5$). Apart from one
 700 location, which had to be fixed before the measurements, the tracer method quantified the A1
 701 and A2 leaks ($n = 8$) and reported an average emission rate of 1.8 L min^{-1} . The tracer method
 702 also quantified all the B and C leaks ($n = 9$) with an average emission rate of 0.1 L min^{-1} .
 703 Mostly due to the safety and time constraints and medium to large underground accumulations
 704 of CH_4 , the suction method could provide incomplete measurements at only 3 locations of A1
 705 and A2 leaks with an average emission rate of 1.5 L min^{-1} ($n = 3$). The suction method measured
 706 at 5 out of 9 B and C locations, one of the measurements was complete and the others were
 707 incomplete, with an average emission rate of 1.0 L min^{-1} ($n = 5$). Although the number of
 708 quantified leaks is limited, all the three methods show that the emission rates from category A1
 709 and A2 leaks are higher than category B and C leaks (Fig. 6). This indicates that the site
 710 selection bias of measurements for the suction method due to safety concerns (see qualifier
 711 above), can lead to a bias in the emission rate in this method.



712

713 **Figure 6 – Emission rate differences between different gas leak categories**

714 4 Discussion

715 4.1 Leak detection methods

716 4.1.1 Leak location vs outlet location

717 There is a difference between the location of the leak in the gas pipeline (leak location; See
 718 Sect. S.7 in SI) and the location where the gas is emitted to the atmosphere (outlet locations;
 719 See Sect. S.2 in SI). Furthermore, a single leak in the gas pipeline can result in multiple
 720 emission outlets at the surface. In this campaign we observed that in most cases (2 out of 18),
 721 the emission outlet at the surface occurred only a few m (sometimes $< 1 \text{ m}$) from the location
 722 of the leak in the gas pipeline. However, in one case, an emission outlet was detected about 60

723 m away from the leak location indicating significant underground gas accumulation and
724 migration (see Fig. 4).

725

726 **4.1.2 Intercomparison of the gas leak detection methods**

727 The mobile method detects atmospheric CH₄ enhancements while measuring continuously with
728 ppb precision from an inlet installed at the front bumper of the car while LDCs apply the carpet
729 method with an instrument precision at the ppm level. High precision for the carpet method is
730 not needed as the inlet to their instruments is connected to a carpet, which is attached to the
731 ground. The mobile method can cover larger areas in shorter times, but not all roads, walkways,
732 or other surface areas where pipelines are buried are accessible with a vehicle. The advantage
733 of the carpet method is that it can precisely follow the pipeline map, which also means that it
734 can locate leaks more precisely. The mobile method use a 10% threshold to neglect unreliable
735 gas leak sources, which sometimes results in neglecting actual signals from small leaks. Also
736 the mobile measurements do not detect all leaks due to the dependence on the wind direction
737 (only downwind sources leaks can be detected). Luetschwager et al. (2021) suggested that 5 to
738 8 plume transects give > 90% probability of gas leak detection at a given location, so if all the
739 streets in an urban area are covered 5 to 8 times, > 90% of the leaks can be detected by mobile
740 measurements.

741 Both the mobile and the carpet method use C₂H₆ signals for distinguishing between fossil and
742 microbial CH₄ emissions, and as for C₂H₆, the instrument used in the mobile method is more
743 sensitive, and faster. In the carpet method, the laboratory analysis of C₂H₆ is slow and with
744 higher detection threshold compared to the mobile method, where C₂H₆ is measured in real-
745 time during the surveys, and also on foot from the emission outlet. The CRDS instrument
746 provides real-time measurements of CH₄ and C₂H₆ at 1 Hz frequency so checking various
747 outlets at a possible gas leak location is faster.

748 At 14 out of the 20 locations in this study, gas leaks were detected (CH₄ signals passing the
749 10% threshold) and quantified with the mobile method. However, we observed that 4 out of 5
750 locations reported by the LDC would not have been detected in mobile surveys without prior
751 information on existence of the leaks because the maximum enhancement was below the
752 mobile detection threshold. At the only location (HH100) from the list of the LDC, where
753 mobile method could quantify the emissions, the outlets were located on the road and the
754 vehicle was driving on top of the outlet. For this location only one of the transects passed the
755 10% enhancement threshold, and the quantification for this location was $\approx 0.7 \text{ L min}^{-1}$, close
756 to the detection threshold of this method, $\approx 0.5 \text{ L min}^{-1}$. One of the other locations, HH101,
757 reported by the LDC had similar surrounding conditions (e.g. presence of buildings, road
758 conditions, etc.) as the other leaks detected by the mobile method, but still the mobile method
759 was not able to detect a gas leak at this location without a priori information from the utility.
760 The quantifications made by the tracer method suggest that the emission rates of the locations
761 provided by the LDC were much lower than the locations detected by mobile measurements
762 (Table 2). The 10% threshold in the mobile method precludes the identification of small leaks
763 ($< 0.5 \text{ L min}^{-1}$), which would only be identified by the carpet method.

764

765 **4.2 Signal attribution in mobile detection method**

766 **4.2.1 Attribution during mobile survey in car**

767 During the mobile measurements we used two approaches to find correlation between CH₄ and
768 C₂H₆. When we compare the online measurements point by point, the probability of detecting
769 a fossil signal is high, as only one single significant reading is sufficient to indicate a fossil
770 signal. When we use the R² of the linear correlation between CH₄ and C₂H₆ enhancements
771 above the cut-off, the attribution is more reliable. In a large dataset without a priori information

772 on the existence of a gas leak at different locations, the correlation method is more trustworthy
773 as the point-by-point method could be affected by instrument noise and/or spikes.
774 We also used CO₂ signals and their correlation with CH₄ signals to investigate interference
775 from combustion or microbial processes. For only 7 plumes at 6 locations, we detected
776 correlations between CO₂ and CH₄, which could indicate either oxidation of CH₄ to CO₂ or
777 mixture of microbial CH₄ emissions from e.g. the sewer system with the emissions from natural
778 gas leaks. The number of these possible co-emissions is low compared to the number of total
779 transects (only $\approx 7\%$ of the plumes with CH₄ enhancements greater than 10%), thus such an
780 admixture of microbial CH₄ should not impact the quantification from mobile method
781 significantly.

782 **4.2.2 Plume attribution to emission outlets**

784 The outlet attribution was performed using the G4302 CRDS instrument which is portable like
785 a backpack. We checked the outlets (See Sect. S.2, Fig. S1) around the locations of interest and
786 evaluated the correlation between CH₄ and C₂H₆ and the persistence of the emissions on
787 different days. In theory, it is possible to estimate contributions of fossil and microbial CH₄ in
788 a plume using the ethane signals during the mobile measurements with the vehicle and the
789 reference C₂:C₁ ratio provided by the LDC. However, due to the low C₂H₆ signals in ambient
790 air, it was not feasible to quantify the possible contribution of microbial methane emissions.
791 Nevertheless, the C₂H₆ signals of the G4302 CRDS instrument were still very useful to identify
792 a location as a possible gas leak location or not. For all the 15 locations, which were initially
793 detected by the mobile method we observed detectable C₂H₆ signals, including the two
794 locations which later were not confirmed as a gas leak location by the LDC. This suggests that
795 either the leak is at a greater distance and depending on the transport of the emission we
796 periodically can see the signals at the detected outlets or that there are sources that produce
797 both CH₄ and C₂H₆ in the vicinity of the location.

799 **4.3 Leak quantification methods**

800 **4.3.1 Mobile method**

801 If the outlets are close to each other, we may observe several CH₄ enhancements close to each
802 other or overlapping when a single transect is performed at a close distance. If we assume that
803 the number of CH₄ maxima is equivalent to the number of real outlets that exist on a road and
804 only use the maximum enhancements from the most pronounced plume to calculate the
805 emission rate, the total emission will be underestimated with the mobile method.

806 Emission rate estimates with the mobile method from individual transects are associated with
807 high uncertainty, related to variabilities in either above-ground or under-ground conditions. For
808 example, an unfavorable wind direction (above ground condition) can result in missing a plume
809 from a gas leak. The mobile measurement van itself may also affect the measurement, e.g., by
810 creating pressure fluctuations. Luetschwager et al. (2021) showed that the quantifications from
811 the same leak in individual mobile transects can vary by more than an order of magnitude. In
812 Hamburg, we found that the range can be even a factor 50 or 100 in exceptional cases (Table
813 2). This high variability illustrates that if we perform only one transect per location, the
814 estimated leak emission rate can result in high under / overestimation in emission estimate for
815 the single location, as was also reported by Maazallahi et al. (2020). This large uncertainty for
816 individual locations is less severe when the results are extrapolated to the city-level, where the
817 sample size is also large, including over- and underestimates (Brandt et al., 2016).

818 In our previous study in Hamburg (Maazallahi et al., 2020) the overall average emission rate
819 for all the LIs was estimated 3.4 L min⁻¹ LI⁻¹ (n = 145) while for the fossil-attributed
820 locations it was 5.2 L min⁻¹ LI⁻¹ (n = 45; standard error of 3.1). This showed that the biggest
821 emitters were among the fossil categories. In the present study, the average emission rate from

822 mobile measurements for the gas leak locations is $2.7 \text{ L min}^{-1} \text{ LI}^{-1}$ ($n = 14$; standard error of
823 0.6). The higher average emission rate per fossil location in the first campaign may have been
824 caused by the fact that in that campaign only a smaller number of transects were performed per
825 location (on average 1.1 in the previous study versus 6.9 transects with $\text{CH}_4 > 10\%$ threshold
826 per location in the present study). Luetschwager et al. (2021) stated that after 6 transects with
827 CH_4 exceeding the 10% threshold per location the average overestimation of leak size estimates
828 will be less than 10%. In addition, the differences in sample size and locations in these two
829 studies (45 versus 14 locations in the first and second studies respectively) may partially
830 explain the difference in average. This is because the probability of detecting large emitters,
831 which increase the average emission rate of all leaks, increases with sample size.

832 The two CH_4 sensors onboard the mobile van play specific roles in the detection and
833 quantification of leaks. CH_4 enhancements on the G2301 are 3.8 times lower than the G4302.
834 This is an artefact of the G2301, which smoothes the signal compared to the G4302 because of
835 the slower pump and sampling rate (See Sect. S.8.1 in SI). On the other hand, this results in
836 more signals passing the 10% threshold on G4302. This then also leads to higher detection
837 probabilities using G4302 (See Sect. S.8.2 in SI). Higher record of CH_4 enhancements then
838 also results in higher emission rate quantification using Eq. 1 (See Sect. S.8.3 in SI). We use
839 the G2301 for quantification, since this is the instrument that was also used for introduction of
840 the mobile equation quantification in Weller et al. (2017). The quantification of the gas leak
841 locations using Eq. 1 depends only on the CH_4 enhancements. This gives about a factor 2 higher
842 emission rates from G4302 than from G2301 for the same plumes. When we evaluate the plume
843 areas from the two instruments, they are much closer to the 1:1 line (See Sect. S.8.3 in SI). This
844 agrees with findings from another study using two different in-situ instruments onboard a
845 mobile car (See Sect. S1.5, Fig. S6 from Ars et al. (2020)). They also found that the plume area
846 is closer to the 1:1 line in mobile measurements even if the air intakes are not at the same
847 location of the vehicle. This suggests that the plume area is a more robust parameter than
848 maximum enhancement for emission rate quantification and a leak rate quantification equation
849 using the plume area should be developed.

850 In general, the closer the air intake is to the emission point the higher the CH_4 mole fraction
851 reading is (See Sect. S.9 in SI), but when several outlets are present at one location it is not
852 possible to uniquely determine the distance to the emission point, and also determine which
853 plume belongs to which outlet. Eq. 1 from Weller et al. (2019) only uses the maximum CH_4
854 enhancements above the 10% threshold from each pass. In their controlled release experiments
855 the average distance between the leak and measurement was 15.75 m. Analysis of our results
856 (Table S4, Sect S.5 in SI) shows that higher maximum concentrations are encountered more
857 often when the distances of the transect to the leak location are small. For example, at HH002
858 the transect was very close to the main emission point, which likely leads to the substantially
859 higher emission rate estimate derived from the mobile method (4.9 L min^{-1}) compared to the
860 tracer method (0.22 L min^{-1}). On the other hand, at HH011 the mobile method underestimates
861 the emission rate (See Sect. 3.3.1), as at this location the measurement distance to the leak was
862 larger than reference distance of 15.75 m applied by Weller et al. (2019). This suggests that to
863 reduce the quantification error for individual leak locations, distance should also be included
864 in an improved transfer equation.

865 The effect of neglecting or retaining the transects with enhancement maxima below the 10%
866 threshold was quantitatively investigated for 5 locations where the tracer team conducted
867 mobile measurements (See Sect. S.10 in SI). These measurements were evaluated as
868 “controlled release” experiments for C_2H_2 , because the actual C_2H_2 release rate is known, and
869 measurements were made in mobile mode. The standard mobile quantification algorithm with
870 the 10% threshold yields emission estimates that are in relatively good agreement with the
871 released quantities, whereas the estimates are biased considerably low when measurements

872 with maxima below the threshold are retained. This supports the use of the original method,
873 which removes transects with an improper realization of the plume. Relating to section 4.5, it
874 must be noted, however that in these measurements the distances of the C₂H₂ maxima to the
875 release points were between 30 to 45 m, thus larger than the normal distance of mobile CH₄
876 measurement to the emission outlets (from few meters up to 30 m).

877

878 **4.3.2 Tracer method**

879 The tracer method is more labor intensive than the mobile method. However, the strength of
880 the method is the application of a tracer gas providing the plume dilution and avoiding the use
881 of atmospheric dispersion models and weather information. If the tracer release location does
882 not reflect the sum of all the outlet emissions at a gas leak location, or misses some of the
883 outlets, then the total emission quantification from the gas leaks will be underestimated. An
884 example of such a case is site HH011 in this study where the leak location in the gas pipeline
885 (after quantification; see Fig. 1) was found to be located about 60 m upwind the targeted
886 emission outlet. During tracer quantification, an additional CH₄ plume (not defined by the
887 tracer gas) was observed indicating more than one emission outlet (Fig. 4). The confirmation
888 for this is the finding of gas leak location by the carpet method. The emission rate of the
889 targeted emission source (the vent and the drain) is thus not representing the combined
890 emission from the gas leak in the pipeline located 60 m upwind the emission source. Further
891 surface screening and leak detection would have been needed to identify and quantify all
892 emission outlets.

893

894 **4.3.3 Suction method**

895 The suction method is the most labor-intensive quantification method. Following a strict, safety
896 first, protocol the gas utilities fix leaks in the A1 safety category immediately upon detection
897 and A2 leaks within a week. Given logistical constraints, the suction method therefore mainly
898 or exclusively quantifies B or C leaks (50% of confirmed gas leak location in this study). We
899 investigated whether such a site selection bias could lead to a bias in the average quantified
900 emission rate in the inventory report. In this study, we observed that the leaks detected from
901 the mobile methods were mostly in the A1 and A2 category and the biggest emitters (based on
902 the mobile and tracer release measurements) had soil CH₄ accumulation of a magnitude that
903 prevented successful application of the suction method. Further research is needed to identify
904 the physical mechanism(s) to explain the observed correlation between A1 and A2 leaks and
905 high emission rates. As a hypothesis, the presence of soil cavities associated with leak category
906 A1 may result in higher permeability, i.e. lower underground resistance, which then leads to
907 higher emission rate for the same pipeline hole size compared to locations with no cavity.

908 The suction method was intended to be deployed right before the repair actions. For some of
909 these locations, the suction method was in operation for more than 10 hours, but due to the high
910 soil CH₄ accumulation, the measurements were stopped and labeled as incomplete in this study.
911 For the other locations with high soil CH₄ accumulation, the suction method was not attempted,
912 given the expectation (based on experience at the incomplete locations) that completion of
913 measurements for leak rate quantification at those locations was unlikely.

914

915 **4.3.4 Hole method**

916 Based on the leak size, pipeline depth and overpressure, the average emission rate was
917 estimated at 40 L min⁻¹ (n = 5). We note that these estimated should be regarded as upper limits
918 since flow restrictions outside the pipe are not included. The emission range of individual gas
919 leaks based on the hole method is between 19 to 150 L min⁻¹ for 1 cm² to 15 cm² hole sizes
920 respectively, larger than any of the measurement-based quantification methods. This method
921 requires information about the overpressure of the gas pipeline, depth of buried pipeline and

922 size of a leak and it does not include the information about soil properties, which can impact
923 the emission rate.

924

925 **4.3.5 Intercomparison of methods**

926 In this study, a reliable quantitative intercomparison of the three methods (mobile, tracer and
927 suction methods) was attempted. A complete comparison of all three methods was possible at
928 only one out of 20 locations (18 confirmed gas leak locations) because of the long time (>8-10
929 hrs) needed for full equilibrium of the suction method, whereby emission rates for 7 out of the
930 8 leaks quantified by the suction method were reported as maxima rather than absolute values
931 (Table 1). At these 7 locations the emission was thus overestimated.

932 In total, the average CH₄ emissions from natural gas pipeline leaks for the same locations where
933 we have quantifications from mobile and tracer methods (n = 13) are 2.8 and 1.2 L min⁻¹
934 respectively. The suction method could only be completed at one location. The average
935 emission rate reported for all the locations from the suction method (high bias due to
936 incomplete measurement) is 1.2 L min⁻¹ (n = 8).

937 The higher emission rates derived with the mobile method are in qualitative agreement with
938 previous studies. Weller et al. (2018) compared quantifications from the mobile measurements
939 described in von Fischer et al. (2017) with the tracer method and surface enclosure method in
940 four US cities. They reported that mobile measurement estimates were ≈ 2.3 L min⁻¹ greater
941 than the tracer method mean estimates of ≈ 3.2 L min⁻¹ (n = 59). This was attributed to the
942 overestimation of small leaks (< 2.4 L min⁻¹) in the mobile measurements method, which we
943 have also discussed above for our dataset. In addition, performance of only a few transects at
944 individual locations also lead to systematically high biased emission rate estimates for higher
945 emission rates (Luetschwager et al., 2021). Indeed, at the locations where we only have one
946 transects with CH₄ enhancements above the 10% threshold, there is an overestimation from
947 mobile method compared to the tracer method. For example, at HH001 (n=1), HH015 (n=1)
948 and HH100 (n=1) the mobile method estimated emissions of a factor 4 higher in comparison
949 to the tracer method. The analysis of Luetschwager (2019) clearly shows that this high bias is
950 reduced when numerous transects are performed. Therefore, we carried out multiple transects
951 to reduce this systematic bias. We note that there are also large differences between the mobile
952 and tracer methods, e.g. HH002 and HH006. We suspect that the very short gas leak location
953 distance to the mobile driving transects can explain partially the difference. Moreover,
954 existence of another leak in the category of A1 at the HH006 location which had to be fixed
955 prior to the tracer method could explain the difference in emission rate magnitude at this
956 location. Nevertheless, the limited number of transects and the 10% threshold can contribute
957 to an overestimation of the average leak rate with the mobile method at an individual location.
958 At the same time, however, the mobile method fails to detect leaks entirely when the leak outlet
959 is located downwind of the mobile van. The fact that the mobile method misses downwind
960 emissions constitutes a method specific factor towards biasing city-wide emissions low, which
961 qualitatively counteracts the high bias above.

962 **4.4 Possible suction method sampling bias with implications for emission inventories**

963 *Following our communications with the emission inventory experts (personal*
964 *communications with Christian Böttcher, 2022), we cannot fully reconstruct the methods*
965 *that are used in the existing national inventory report to establish the emission factors due*
966 *to lack of transparency. However, the German environmental agency (UBA) is considering*
967 *to use the results of the recent large scale measurement campaign based on the suction*
968 *method (MEEM, 2018) in future publications of the national emission inventory in Germany*
969 *(Federal Environment Agency, 2021). The utilities choose leak locations for application of*
970 *the suction method where there are no safety concerns and/or immediate leak closure is*
971 *compulsory. This implies that this method is not applied at locations of the A1 category, which*

972 demand immediate repair (P. 27 in *MEEM*, 2018). Due to logistic constraints and the time-
973 consuming nature of the suction measurements, they are likely also not (or rarely) applied at
974 locations in the A2 category, which require repair within a week. Thus, suction measurements
975 have a location sampling bias towards leaks in the B and C category. This is supported by the
976 fact that the leak locations that were contributed by the LDC to the intercomparison campaign
977 were locations in the B and C category. This study investigated whether this location sampling
978 bias could result in an emission rate bias, which could contribute to the fact that the suction
979 method did not report leaks with emission rates as high as they have been reported by the
980 mobile method in this study or during previous measurements in the same city (Maazallahi et
981 al., 2020).

982 In this study, emission rates from A1 and A2 category leaks were larger compared to those
983 from B and C category leaks (Figure 6). The emission rate differences vary by measurement
984 method: a factor 2 for the mobile method (n = 9 for A1&A2, n = 4 for B&C), a factor 11 for
985 the tracer method (n = 8 for A1&A2, n = 8 for B&C) and a factor 1.6 for the suction method
986 (n=3 for A1&A2, n = 5 B&C). For the mobile method, there is a clear separation between the
987 A1&A2 versus the B&C categories. The highest emission estimate for the B&C group
988 (HH010) is similar to the lowest emission rate estimate for the A1&A2 group (HH014).
989 Furthermore, HH011 in the A1 category was very likely biased low because of the wrongly
990 assumed leak location.

991 For the tracer method, the difference between the two groups is largest, an order of magnitude,
992 and we know that emissions are underestimated at least at one location of the A1 category
993 (HH011). The uncertainty of the tracer method is much smaller than the difference between the
994 two groups. The tracer method also illustrates that 4 of the 5 leaks that were contributed by the
995 LDC to the intercomparison campaign were extremely small. If these would be representative
996 for locations where the suction method is usually applied, it would indeed indicate a severe
997 emission rate bias for the suction method, not because the measurements themselves are biased,
998 but because locations with low emission rates are targeted with this method. In the
999 intercomparison campaign, we attempted to apply the suction method also at locations of the
1000 A categories, but at 8 out of 9 locations from the A category, the suction measurements could
1001 not be applied for safety reasons, or suction could not be completed, because of the widespread
1002 subsurface accumulation (Table 2). At the other A location (HH014), the suction method could
1003 not be applied as the ground had been already opened for the repair.
1004

1005 5 Conclusion

1006
1007 In summer 2020, we compared three gas leak rate quantification methods, namely the mobile,
1008 tracer, and suction methods, in Hamburg, Germany. *While the mobile and tracer methods
1009 have been compared previously, this is the first peer-reviewed study that includes the suction
1010 method, although suction measurements could not be completed in one day at most locations.*

1011 The mobile method can cover large areas in a short time, but some of the smaller leaks (< 0.5
1012 L min⁻¹) are not identified as a gas leak location due to the 10% enhancement threshold in the
1013 standard mobile quantification algorithm. While the mobile method quantification algorithm is
1014 designed to accurately report city-level total gas distribution leak rates (i.e., considering a large
1015 sample size), it has large (known) uncertainties for individual leaks. The tracer method has a
1016 smaller uncertainty, but it is labor intensive in comparison to the mobile method. On average,
1017 CH₄ emissions from natural gas pipeline leaks were higher from mobile quantifications in
1018 comparison to tracer quantifications. For many locations, we encountered several outlets and
1019 with widespread underground gas accumulations. At one location, after deployment of the
1020 mobile and the tracer quantification and during the repair actions, it was found out that the

1021 actual leak in the gas pipeline was located ≈ 60 m away from the identified emission outlet
1022 indicating significant underground gas migration. It is possible that this leak had several
1023 emission outlets that were not identified and the emission quantified from the single outlet is
1024 thus not representative for the whole emission from this leak.

1025 The suction method has a low reported uncertainty, but it is even more labor and time intensive
1026 than the tracer method. Due to the time and effort needed to plan and execute the measurements,
1027 the suction method is likely never applied in routine operation at A1 or A2 safety category
1028 leaks that mandate immediate or near-time repair. In our study, it was also not feasible to apply
1029 the suction method at locations with large subsurface CH₄ accumulations. Our results thus
1030 indicate a systematic difference between A1 and A2 (high emissions) versus B and C (low
1031 emissions) category locations, and generally larger emission rates are inferred with the mobile
1032 and tracer methods for sites with widespread subsurface accumulation.

1033 This study did not allow a direct, quantitative comparison of emission rates estimated with all
1034 three different methods because of the inability to quantify the same leak locations with all
1035 methods. However, this inability illuminates the importance of site selection for deriving
1036 representative emission factors based on empirical measurements. Specifically, the results
1037 suggest that a significant emission rate bias could exist for measurements that are carried out
1038 with the suction method. Our results therefore stipulate that representative site selection
1039 includes sampling at all leak safety categories (*MEEM, 2018*). Otherwise, this could lead to a
1040 sampling and emission rate bias in the national inventory of gas leak CH₄ emission in Germany.

1041
1042 **Authors contributions:** TR, HM and SS conceived and designed the study. TR coordinated
1043 the campaign in collaboration with DBI, Technical University of Denmark (DTU),
1044 Environmental Defense Fund (EDF), E.On and Gasnetz Hamburg (GNH) teams. HM carried
1045 out the mobile measurements, emission outlet attribution, performed the analyses of mobile
1046 data and collectively with TR analyzed the intercomparison results. AD, CS and AMF
1047 performed the tracer method and reported the emission rates from the tracer dataset.
1048 HDvdG and TR made instruments and equipment available for the mobile method and CS
1049 provided those for the tracer method. HM wrote the paper, and all co-authors supported the
1050 interpretation of the results and contributed to improving the paper.

1051
1052 **Competing interests:** The authors declare that they have no conflict of interest.

1053 1054 **Acknowledgement**

1055 This study was carried out with the financial support from the Environmental Defense Fund.
1056 Extra financial supports were provided by the H2020 Marie Skłodowska-Curie actions through
1057 Methane goes Mobile – Measurements and Modelling project (MEMO²; [https://h2020-](https://h2020-memo2.eu/)
1058 [memo2.eu/](https://h2020-memo2.eu/), last access: 20 April 2022), grant number 722479. In this study, Robertson
1059 Foundation supported contribution of Stefan Schwietzke. We appreciate efforts from
1060 Luise Westphal, Michael Dammann, Ralf Luy, Christian Feickert, Volker Krell, Turhan Ulas,
1061 Dieter Bruhns and Sönke Graumann, from GasNetz Hamburg GmbH who facilitated this study
1062 by hosting the teams, arranging and applying the carpet method leak detection and confirmation
1063 procedures, making information on gas leaks and pipelines available for the data analysis and
1064 applying leak repair protocols. We extend our appreciation to Andre Lennartz, Stefan Gollanek
1065 and Dieter Wolf from E.On-for their contribution in the planning of the campaign, deploying
1066 the suction method at the locations, and exchanging their knowledge and experiences from
1067 their previous campaigns. We thank the team from DBI Gas and Environmental
1068 Technologies GmbH Leipzig (DBI GUT Leipzig) including Charlotte Große, who contributed
1069 in providing information for structuring the campaign planning.

1070

1071

1072

Reference:

1073 Alvarez, R. A., Pacala, S. W., Winebrake, J. J., Chameides, W. L., Hamburg, S. P.: Greater
1074 focus needed on methane leakage from natural gas infrastructure, PNAS, 109 (17)
1075 6435-6440, <https://doi.org/10.1073/pnas.1202407109>, 2012.

1076 Ars, S., Vogel, F., Arrowsmith, C., Heerah, S., Knuckey, E., Lavoie, J., Lee, C., Mostafavi Pak,
1077 N., Phillips, J. L., and Wunch, D., Investigation of the Spatial Distribution of Methane
1078 Sources in the Greater Toronto Area Using Mobile Gas Monitoring Systems, Environ.
1079 Sci. Technol., 54, 24, 15671–15679, <https://doi.org/10.1021/acs.est.0c05386>, 2020.

1080 Allwine G., Lamb B., Westberg H., Application of Atmospheric Tracer Techniques for
1081 Determining Biogenic Hydrocarbon Fluxes from an Oak Forest. In: Hutchison B.A.,
1082 Hicks B.B. (eds) The Forest-Atmosphere Interaction. Springer, Dordrecht.
1083 https://doi.org/10.1007/978-94-009-5305-5_23, 1985.

1084 Arnaldos, J., Casal, J., Montiel, H., Sánchez-Carricondo, M., Vílchez, J.A., Design of a
1085 computer tool for the evaluation of the consequences of accidental natural gas releases
1086 in distribution pipes, Journal of Loss Prevention in the Process Industries,
1087 [https://doi.org/10.1016/S0950-4230\(97\)00041-7](https://doi.org/10.1016/S0950-4230(97)00041-7), 1998.

1088 Bousquet, P., Ciais, P., Miller, J. B., Dlugokencky, E. J., Hauglustaine, D. A., Prigent, C., Van
1089 der Werf, G. R., Peylin, P., Brunke, E. G., Carouge, C., Langenfelds, R. L., Lathière,
1090 J., Papa, F., Ramonet, M., Schmidt, M., Steele, L. P., Tyler, S. C., White, J.,
1091 Contribution of anthropogenic and natural sources to atmospheric methane variability.
1092 Nature.; 443(7110):439-43. <https://doi.org/10.1038/nature05132>, 2006.

1093 Brandt, A. R., Heath, G. A., and Cooley, D., Methane Leaks from Natural Gas Systems Follow
1094 Extreme Distributions, Environmental Science & Technology, 50 (22), 12512-12520,
1095 <https://doi.org/10.1021/acs.est.6b04303>, 2016

1096 Cho, Y., Ulrich, B. A., Zimmerle, D. J., Smits, K. M., Estimating natural gas emissions from
1097 underground pipelines using surface concentration measurements, Environmental
1098 Pollution, <https://doi.org/10.1016/j.envpol.2020.115514>, 2020.

1099 Defratyka, S. M., Paris, J. D., Yver-Kwok, C., Fernandez, J. M., Korben, P., and Bousquet, P.,
1100 Environmental Science & Technology Article ASAP,
1101 <https://doi.org/10.1021/acs.est.1c00859>, 2021.

1102 Delre, A., Greenhouse gas emissions from wastewater treatment plants: measurements and
1103 carbon footprint assessment, Ph.D. Thesis, Department of Environmental Engineering,
1104 Technical University of Denmark (DTU), Copenhagen, Available at:
1105 <https://orbit.dtu.dk/en/publications/greenhouse-gas-emissions-from-wastewater-treatment-plants-measure>
1106 (Last Accessed: 15 June 2021), 2018.

1107 DVGW: High-performing infrastructure, (2022). [online] Available from
1108 <https://www.dvgw.de/english-pages/topics/safety-and-security/technical-safety-gas>,
1109 (Last Accessed: 25 January 2022)

1110 DVGW: Technische Regel-Arbeitsblatt; DVGW G465-1 (A) (2019). [online] Available from:
1111 https://shop.wvgw.de/var/assets/leseprobe//510544_lp_G_465-1_2019_05.pdf. (Last
1112 Accessed: 15 December 2021)

1113 Ebrahimi-Moghadam, A., Farzaneh-Gord, M., Arabkoohsar, A., Jabari Moghadam, A., CFD
1114 analysis of natural gas emission from damaged pipelines: Correlation development for
1115 leakage estimation, Cleaner Production, <https://doi.org/10.1016/j.jclepro.2018.07.127>,
1116 2018.

1117 EC: EU strategy to reduce methane emissions available at: <https://eur-lex.europa.eu/legal-content/EN/TXT/?uri=CELEX%3A52020DC0663&qid=1644853088591>,
1118 (last
1119 access: 28 March 2022), 2020

1120 EIA, Carbon Dioxide Emissions Coefficients , available at:
1121 https://www.eia.gov/environment/emissions/co2_vol_mass.php, (last access:
1122 28 March 2022), 2021.

1123 EPA, Methane emissions from the natural gas industry: underground pipelines,
1124 https://www.epa.gov/sites/production/files/2016-08/documents/9_underground.pdf,
1125 1996.

1126 Federal Environment Agency: National Inventory Report for the German Greenhouse Gas
1127 Inventory 1990–2019, available at: <https://unfccc.int/documents/194930>, (last access:
1128 15 December 2022), 2021.

1129 Fernandez, J. M., Maazallahi, H., France, J. L., Menoud, M., Corbu, M., Ardelean, M., Calcan,
1130 A., Townsend-Small, A., van der Veen, C., Fisher, R. E., Lowry, D., Nisbet, E.G.,
1131 Röckmann, T.: Street-level methane emissions of Bucharest, Romania and the
1132 dominance of urban wastewater., *Atmospheric Environment: X*, 13, 2590-1621,
1133 100153, <https://doi.org/10.1016/j.aeaoa.2022.100153>, 2022.

1134 Fredenslund, A.M., Scheutz, C., Kjeldsen, P.: Tracer method to measure landfill gas emissions
1135 from leachate collection systems, *Waste Management*, 30, 2146-2152,
1136 <https://doi.org/10.1016/j.wasman.2010.03.013>, 2010

1137 Fredenslund, A. M., Rees-White, T. C., Beaven, R. P., Delre, A., Finlayson, A., Helmore, J.,
1138 Allen, G., Scheutz, C.: Validation and error assessment of the mobile tracer gas
1139 dispersion method for measurement of fugitive emissions from area sources, *Waste
1140 Management*, 83, 68-78, <https://doi.org/10.1016/j.wasman.2018.10.036>, 2019.

1141 Federal Environment Agency: National Inventory Report for the German Greenhouse Gas
1142 Inventory 1990 – 2018, available at: <https://unfccc.int/documents/226313> (last access:
1143 30 March 2022), 2020.

1144 Hendrick, M. F., Ackle, R., Sanaie-Movahed, B., Tang, X., Phillips, N. G., Fugitive methane
1145 emissions from leak-prone natural gas distribution infrastructure in urban
1146 environments, *Environmental Pollution*, <https://doi.org/10.1016/j.envpol.2016.01.094>,
1147 2016.

1148 Hou, Q., Yang, D., Li, X., Xiao, G. and Ho, S. C. M., Modified Leakage Rate Calculation
1149 Models of Natural Gas Pipelines, *Mathematical Problems in Engineering*,
1150 <https://doi.org/10.1155/2020/6673107>, 2020.

1151 Jackson, R. B., Saunio, M., Bousquet, P., Canadell, J. G., Poulter, B., Stavert, A. R.,
1152 Bergamaschi, P., Niwa, Y., Segers, A. and Tsuruta, A., Increasing anthropogenic
1153 methane emissions arise equally from agricultural and fossil fuel sources,
1154 *Environmental Research Letters*, 15, 071002, [https://doi.org/10.1088/1748-
1155 9326/ab9ed2](https://doi.org/10.1088/1748-9326/ab9ed2), 2020.

1156 Jackson, R. B., Down, A., Phillips, N. G., Ackley, R. C., Cook, C. W., Plata, D. L., and Zhao,
1157 K., Natural Gas Pipeline Leaks Across Washington, DC, *Environ. Sci. Technol.*, 48, 3,
1158 2051–2058, <https://doi.org/10.1021/es404474x>, 2014.

1159 Kirchgessner, D. A., Lott R. A., Cowgill, R.M., Harrison, M. R., Shires, T. M., Estimate of
1160 methane emissions from the U.S. natural gas industry, *Chemosphere*,
1161 [https://doi.org/10.1016/S0045-6535\(97\)00236-1](https://doi.org/10.1016/S0045-6535(97)00236-1), 1997.

1162 Keyes, T., Ridge G., Klein, M., Phillips, N., Ackley, R., Yang Y., An enhanced procedure for
1163 urban mobile methane leak detection. *Heliyon*. 9; 6 (10):e04876.
1164 <https://doi.org/10.1016/j.heliyon.2020.e04876>, 2020.

1165 Lamb, B. K., McManus, J. B., Shorter, J. H., Kolb, C. E., Mosher, B., Harriss, R. C., Allwine,
1166 E., Blaha, D., Howard, T., Guenther, A., Lott, R. A., Siverson, R., Westburg, H., and
1167 Zimmerman, P., Development of atmospheric tracer methods to measure methane
1168 emissions from natural gas facilities and urban areas, *Environmental Science &
1169 Technology* 29 (6), 1468-1479 <https://doi.org/10.1021/es00006a007>, 1995.

1170 Lamb, B. K., Edburg, S. L., Ferrara, T. W., Howard, T., Harrison, M. R., Kolb, C. E.,
1171 Townsend-Small, A., Dyck, W., Possolo, A., and Whetstone, J. R., *Environmental*
1172 *Science & Technology* 49 (8), 5161-5169 <https://doi.org/10.1021/es505116p>, 2015.

1173 Luetschwager, E., von Fischer, J. C., Weller, Z. D., Characterizing detection probabilities of
1174 advanced mobile leak surveys: Implications for sampling effort and leak size estimation
1175 in natural gas distribution systems. *Elementa: Science of the Anthropocene*; 9 (1):
1176 00143. <https://doi.org/10.1525/elementa.2020.00143>, 2021.

1177 Liu, C., Liao, Y., Liang, J., Cui, Z., Li, Y., Quantifying methane release and dispersion
1178 estimations for buried natural gas pipeline leakages, *Process Safety and Environmental*
1179 *Protection*, <https://doi.org/10.1016/j.psep.2020.11.031>, 2021.

1180 Maazallahi, H., Fernandez, J. M., Menoud, M., Zavala-Araiza, D., Weller, Z. D., Schwietzke,
1181 S., von Fischer, J. C., Denier van der Gon, H., and Röckmann, T.: Methane mapping,
1182 emission quantification, and attribution in two European cities: Utrecht (NL) and
1183 Hamburg (DE), *Atmos. Chem. Phys.*, 20, 14717–14740, [https://doi.org/10.5194/acp-](https://doi.org/10.5194/acp-20-14717-2020)
1184 [20-14717-2020](https://doi.org/10.5194/acp-20-14717-2020), 2020.

1185 Mahgerefteh, H., Oke, A., Atti, O., Modelling outflow following rupture in pipeline networks,
1186 *Chemical Engineering Science*, <https://doi.org/10.1016/j.ces.2005.10.013>, 2006.

1187 MEEM, Methane emission estimation method for the gas distribution grid, [Online], Available
1188 from: [https://www.dbi-](https://www.dbi-gut.de/emissions.html?file=files/PDFs/Emissionen/Final%20Report_MEEM%20DSO_end_signed.pdf&cid=5804)
1189 [gut.de/emissions.html?file=files/PDFs/Emissionen/Final%20Report_MEEM%20DSO](https://www.dbi-gut.de/emissions.html?file=files/PDFs/Emissionen/Final%20Report_MEEM%20DSO_end_signed.pdf&cid=5804)
1190 [_end_signed.pdf&cid=5804](https://www.dbi-gut.de/emissions.html?file=files/PDFs/Emissionen/Final%20Report_MEEM%20DSO_end_signed.pdf&cid=5804). (Last Accessed: 12 December 2022), 2018.

1191 Moloudi, R., Abolfazli Esfahani, J., Modeling of gas release following pipeline rupture:
1192 Proposing non-dimensional correlation, *Journal of Loss Prevention in the Process*
1193 *Industries*, <https://doi.org/10.1016/j.jlp.2014.09.003>, 2014.

1194 Mønster, J. G., Samuelsson, J., Kjeldsen, P., Rella, C. W., Scheutz, C., Quantifying methane
1195 emission from fugitive sources by combining tracer release and downwind
1196 measurements – A sensitivity analysis based on multiple field surveys, *Waste*
1197 *Management*, 34, 1416-1428, <https://doi.org/10.1016/j.wasman.2014.03.025>, 2014.

1198 Myhre, G., Shindell, D., Bréon, F. M., Collins, W., Fuglestad, J., Huang, J., Koch, D.,
1199 Lamarque, J. F., Lee, D., Mendoza, B., Nakajima, T., Robock, A., Stephens, G.,
1200 Takemura, T., and Zhan, H.: Anthropogenic and Natural Radiative Forcing, in:
1201 *Climate Change 2013: The Physical Science Basis, Contribution of Working Group I*
1202 *to the Fifth Assessment Report of the Intergovernmental Panel on Climate Change*,
1203 Cambridge, UK and New York, NY, USA, available at:
1204 https://www.ipcc.ch/site/assets/uploads/2018/02/WG1AR5_Chapter08_FINAL.pdf,
1205 2013.

1206 Nisbet, E. G., Manning, M. R., Dlugokencky, E. J., Fisher, R. E., Lowry, D., Michel, S. E.,
1207 Myhre, C. L., Platt, S. M., Allen, G., Bousquet, P., Brownlow, R., Cain, M., France, J.
1208 L., Hermansen, O., Hossaini, R., Jones, A. E., Levin, I., Manning, A. C., Myhre, G.,
1209 Pyle, J. A., Vaughn, B. H., Warwick, N. J., White, J. W. C., Very strong atmospheric
1210 methane growth in the 4 Years 2014–2017: implications for the Paris agreement, *Global*
1211 *Biogeochemical Cycles*, 33, 318 – 342, <https://doi.org/10.1029/2018GB006009>, 2019.

1212 Okamoto, H., Gomi, Y., Empirical research on diffusion behavior of leaked gas in the ground,
1213 *Journal of Loss Prevention in the Process Industries*,
1214 <https://doi.org/10.1016/j.jlp.2011.01.007>, 2011.

1215 Phillips, N. G., Ackley, R., Crosson, E. R., Down, A., Hutyra, L. R., Brondfield, M., Karr, J.
1216 D., Zhao, K., Jackson, R. B., Mapping urban pipeline leaks: Methane leaks across
1217 Boston, *Environmental Pollution*, 173, 1–4,
1218 <https://doi.org/10.1016/j.envpol.2012.11.003>, 2013.

1219 Scheutz, C., Samuelsson, J., Fredenslund, A.M., Kjeldsen, P., Quantification of multiple
1220 methane emission sources at landfills using a double tracer technique, *Waste*
1221 *Management*, 31, 1009-1017, <https://doi.org/10.1016/j.wasman.2011.01.015>, 2011.

1222 Ulrich, B. A., Mitton, M., Lachenmeyer, E., Hecobian, A., Zimmerle, D., and Smits, K. M.,
1223 Natural Gas Emissions from Underground Pipelines and Implications for Leak
1224 Detection, *Environmental Science & Technology Letters*, 6 (7), 401-406,
1225 <https://doi.org/10.1021/acs.estlett.9b00291>, 2019.

1226 Von Fischer, J. C., Cooley, D., Chamberlain, S., Gaylord, A., Griebenow, C. J., Hamburg, S.
1227 P., Salo, J., Schumacher, R., Theobald, D., and Ham, J.: Rapid, Vehicle-Based
1228 Identification of Location and Magnitude of Urban Natural Gas Pipeline Leaks,
1229 *Environ. Sci. Technol.*, 51, 4091–4099, <https://doi.org/10.1021/acs.est.6b06095>, 2017.

1230 Weller, Z. D., Roscioli, J. R., Daube, W. C., Lamb, B. K., Ferrara, T. W., Brewer, P. E., and
1231 von Fischer, J. C.: Vehicle-Based Methane Surveys for Finding Natural Gas Leaks and
1232 Estimating Their Size: Validation and Uncertainty, *Environ. Sci. Technol.*, 52, 11922–
1233 11930, <https://doi.org/10.1021/acs.est.8b03135>, 2018.

1234 Weller, Z. D., Yang, D. K., and von Fischer, J. C.: An open source algorithm to detect natural
1235 gas leaks from mobile methane survey data, edited by: Mauder, M., *PLoS One*, 14,
1236 e0212287, <https://doi.org/10.1371/journal.pone.0212287>, 2019.

1237 Weller, Z. D., Hamburg, S. P., and von Fischer, J. C., A National Estimate of Methane Leakage
1238 from Pipeline Mains in Natural Gas Local Distribution Systems, *Environmental*
1239 *Science & Technology*, 54 (14), 8958-8967, <https://doi.org/10.1021/acs.est.0c00437>,
1240 2020

1241 Wiesner, S., Gröngröft, A., Ament, F. et al. Spatial and temporal variability of urban soil water
1242 dynamics observed by a soil monitoring network. *J Soils Sediments* 16, 2523–2537.
1243 <https://doi.org/10.1007/s11368-016-1385-6>, 2016

1244 Worden, J. R., Anthony Bloom, A., Pandey, S., Jiang, Z., Worden, H. M., Walker, T. W.,
1245 Houweling, S., Röckmann, T., , Reduced biomass burning emissions reconcile
1246 conflicting estimates of the post-2006 atmospheric methane budget, *Nature*
1247 *Communications* 8, 2227 <https://doi.org/10.1038/s41467-017-02246-0>, 2017

1248 Yan, Y., Dong, X., Li, J., Experimental study of methane diffusion in soil for an underground
1249 gas pipe leak, *Journal of Natural Gas Science and Engineering*,
1250 <https://doi.org/10.1016/j.jngse.2015.08.039>, 2015.

1251 Yuhua, D., Huilin, G., Jing'en, Z., Yaorong, F., Evaluation of gas release rate through holes in
1252 pipelines, *Journal of Loss Prevention in the Process Industries*,
1253 [https://doi.org/10.1016/S0950-4230\(02\)00041-4](https://doi.org/10.1016/S0950-4230(02)00041-4), 2002.

1254